# Supplementary Information

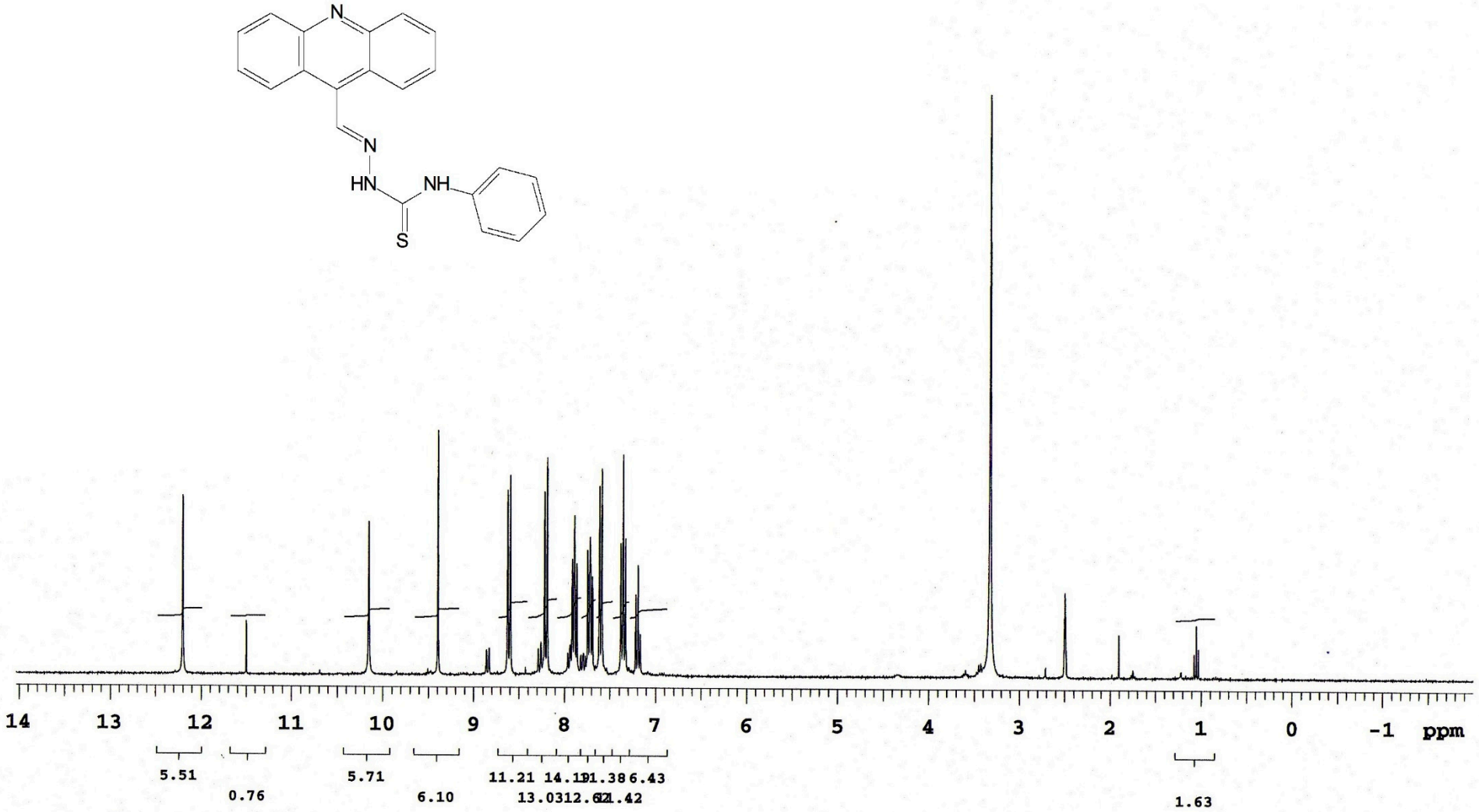


**Figure S1.** $^{1}$H-NMR spectrum (DMSO) of derivative **3a**.

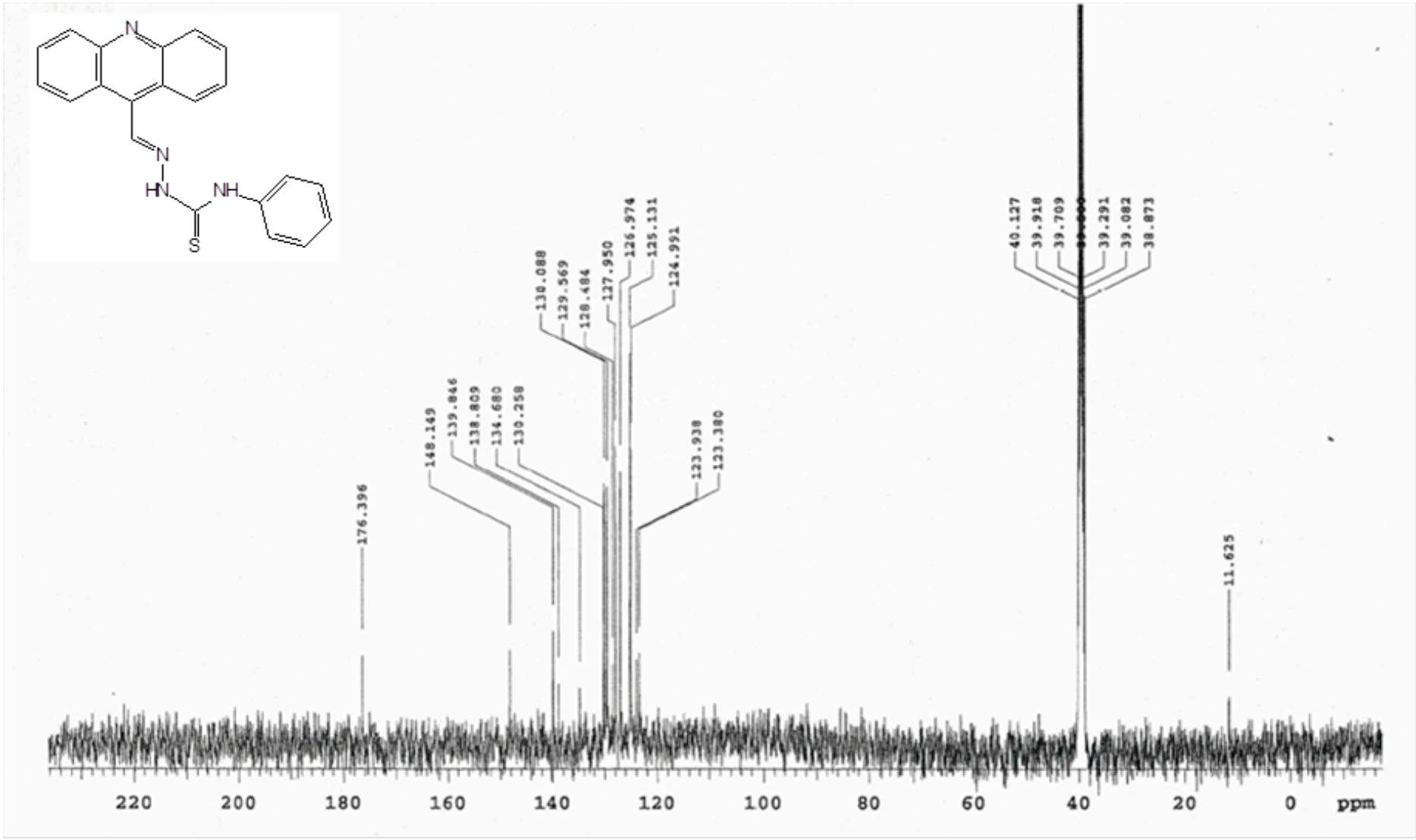


**Figure S2.** $^{13}$C-NMR spectrum (DMSO) of derivative **3a**.

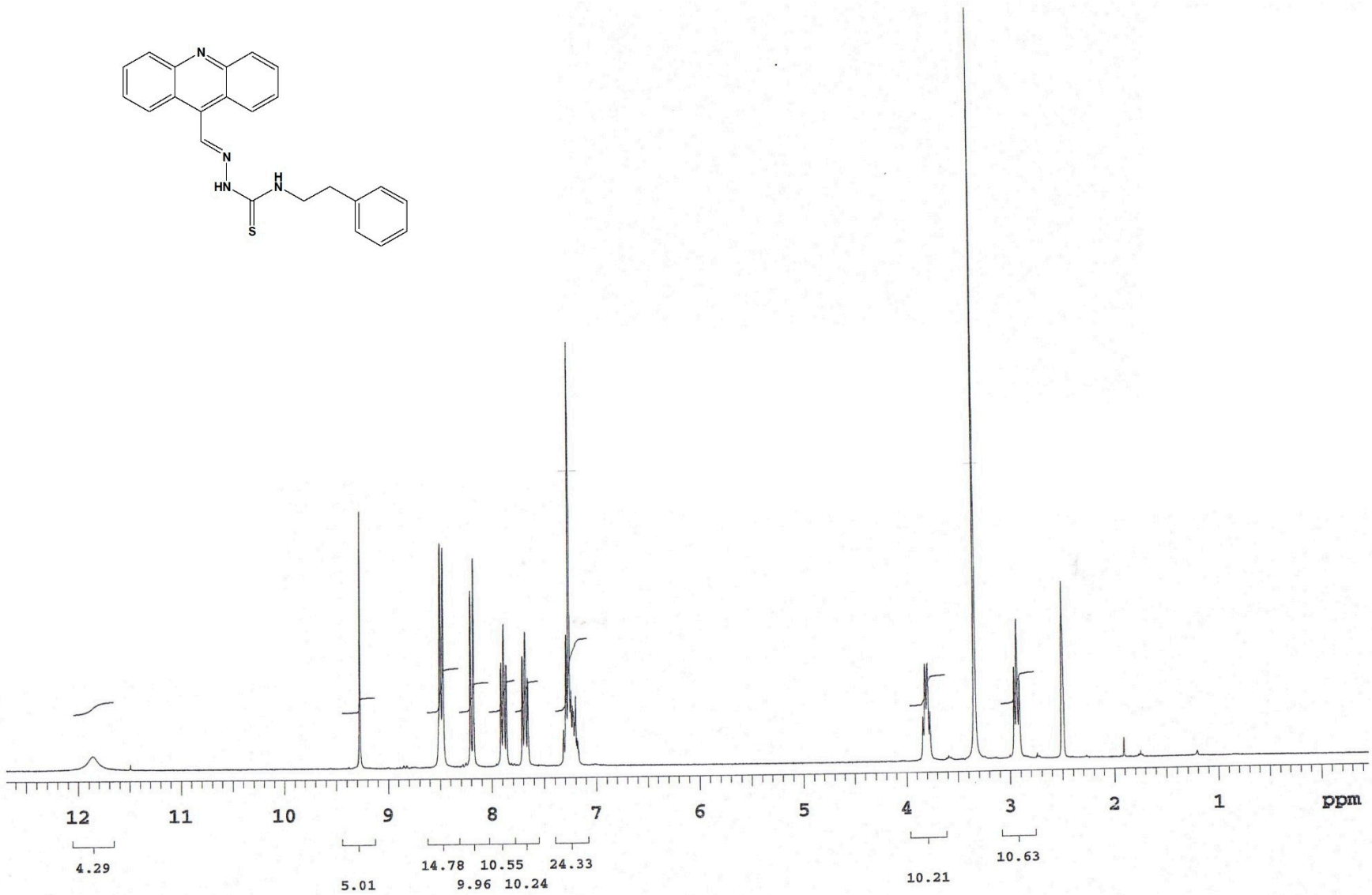


**Figure S3.** $^{1}$H-NMR spectrum (DMSO) of derivative **3b**.

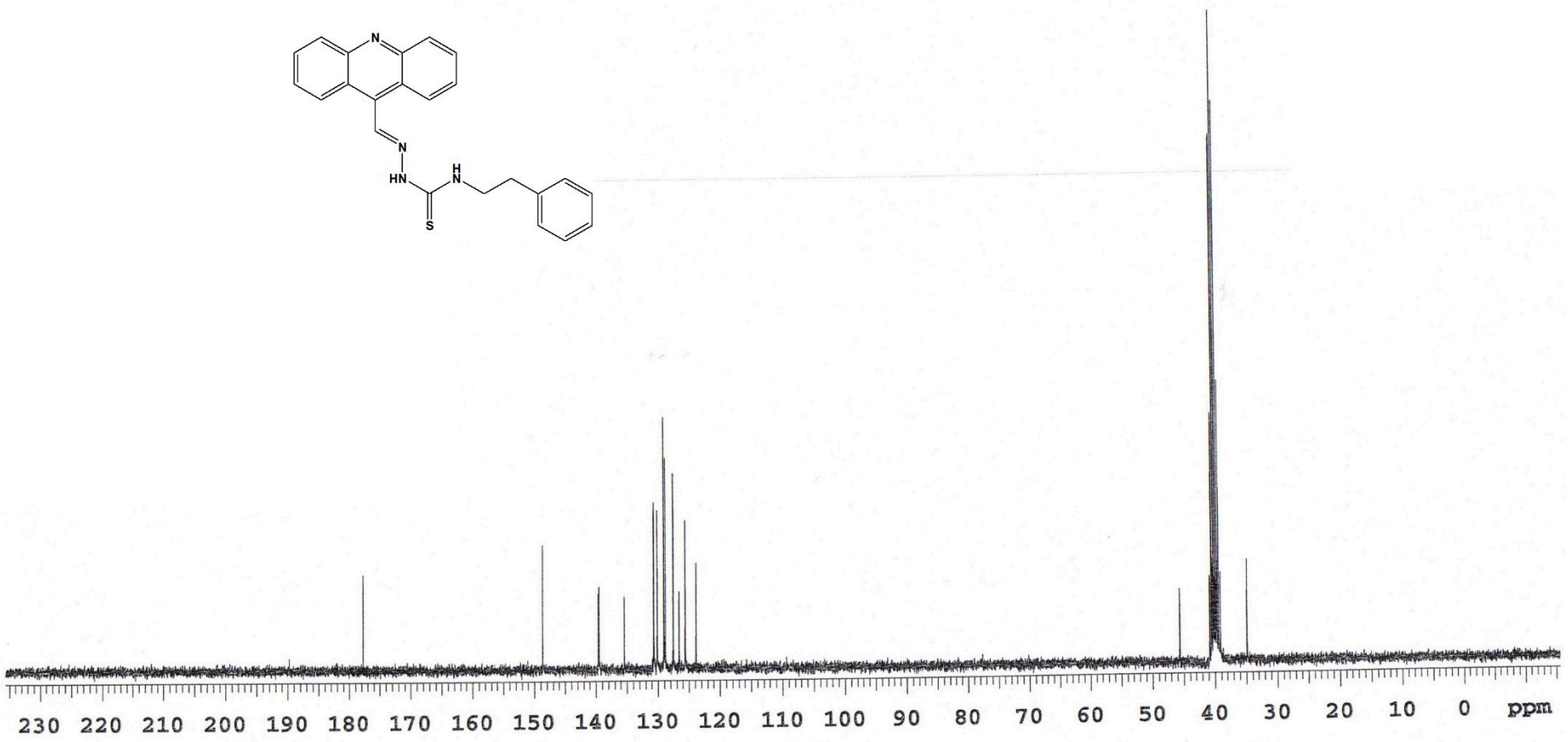


**Figure S4.** $^{13}$C-NMR spectrum (DMSO) of derivative **3b**.

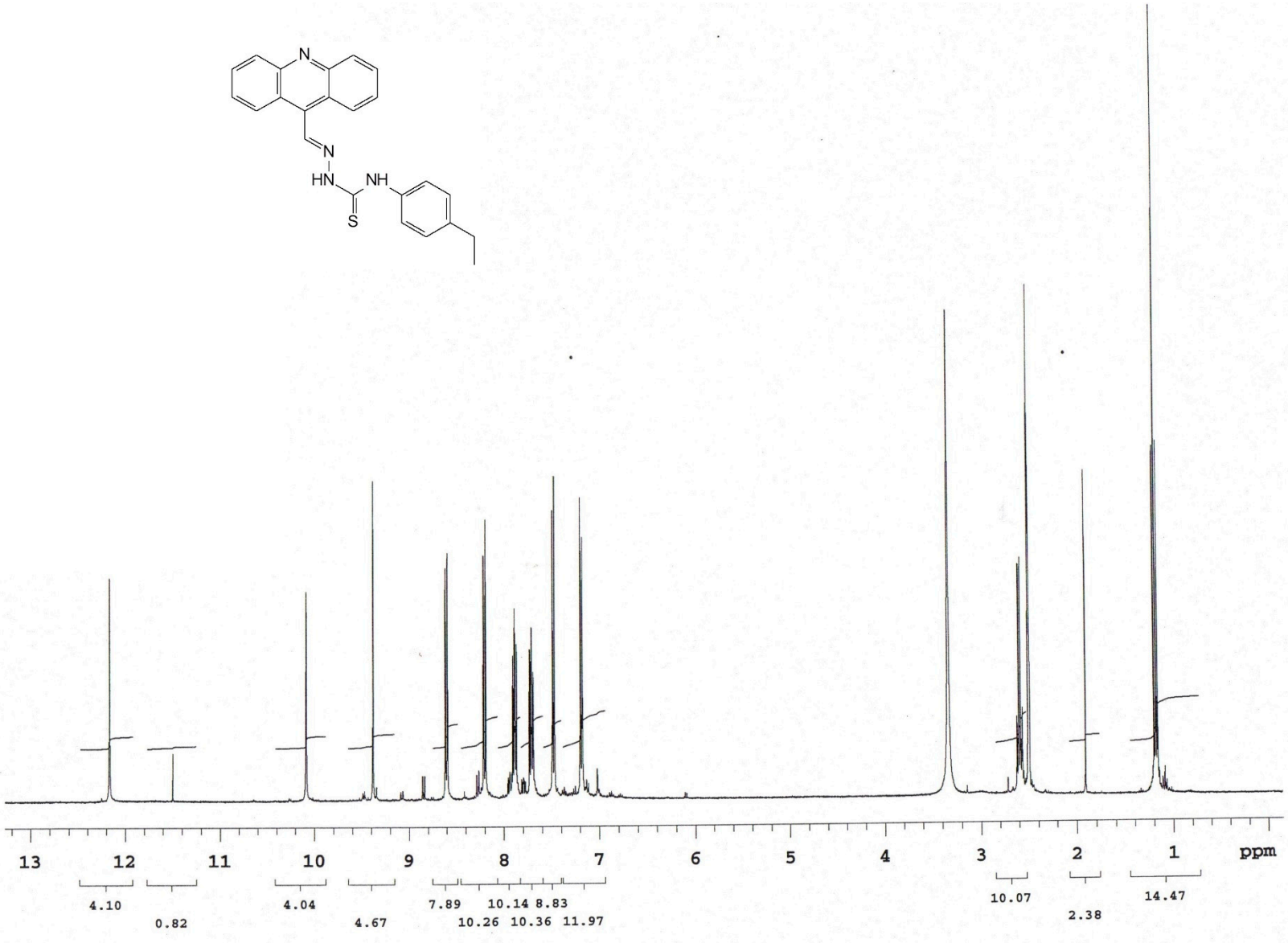


**Figure S5.** $^{1}$H-NMR spectrum (DMSO) of derivative **3c**.

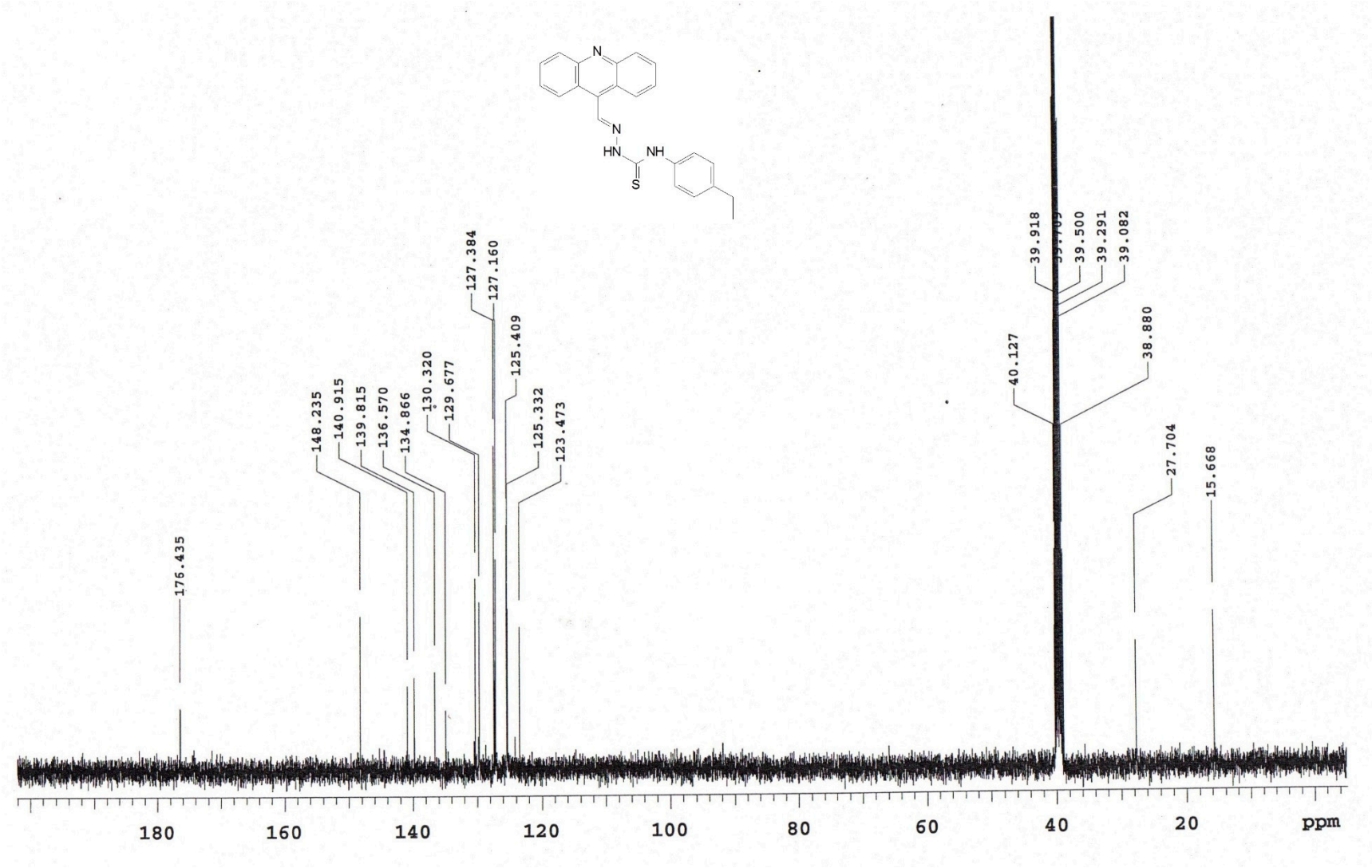


**Figure S6.** $^{13}$C-NMR spectrum (DMSO) of derivative **3c**.

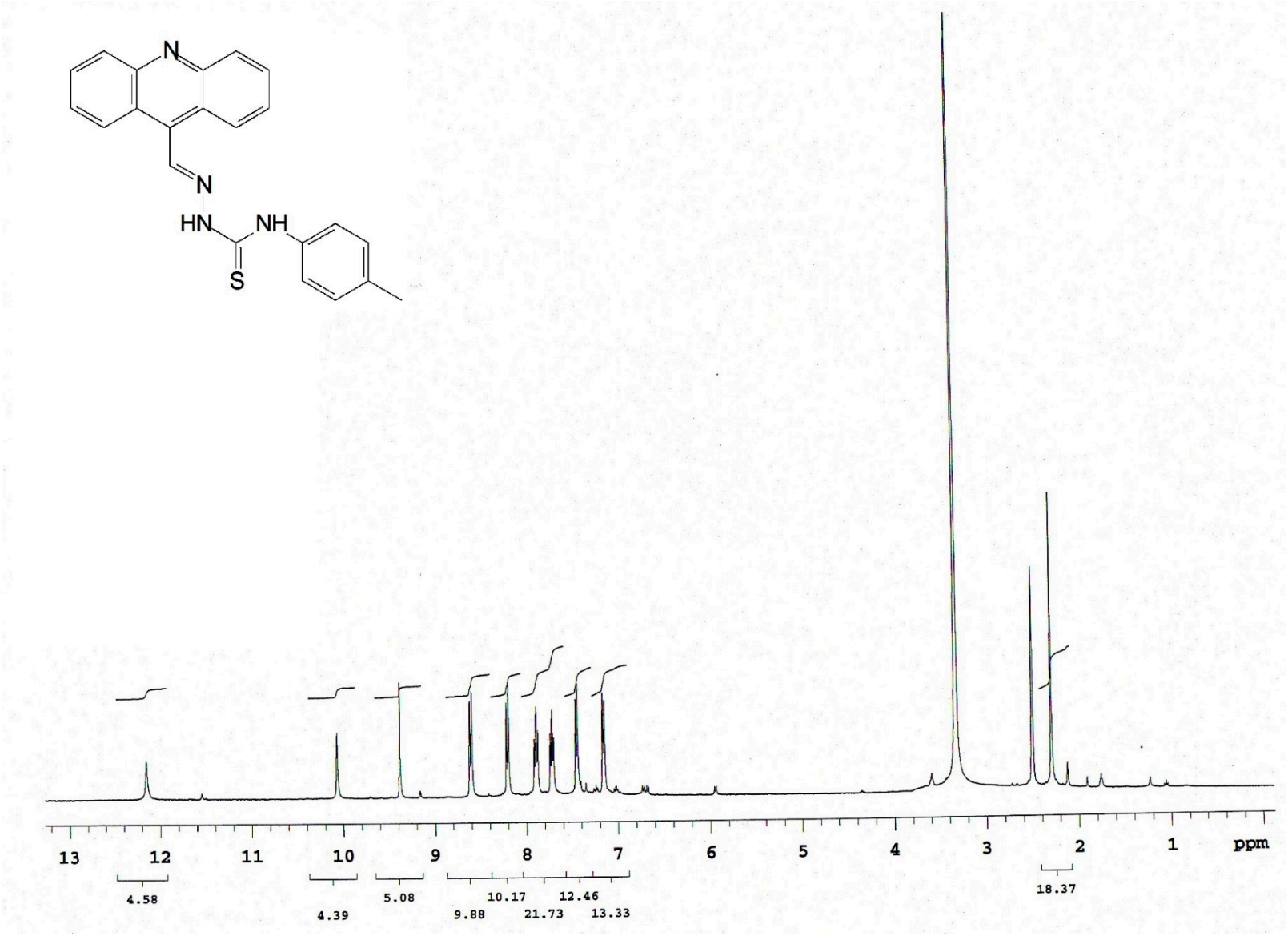


**Figure S7.** $^{1}$H-NMR spectrum (DMSO) of derivative **3d**.

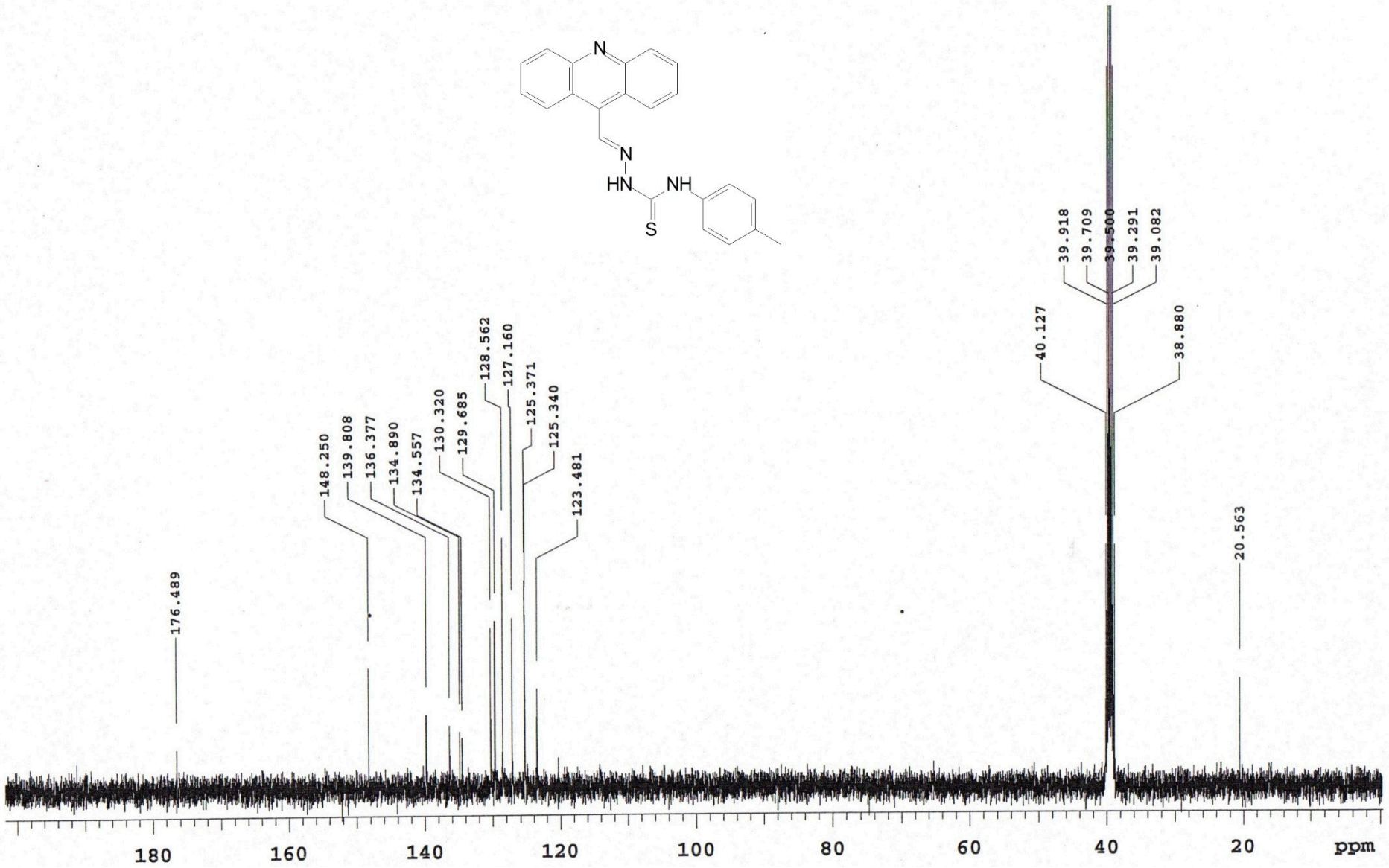


**Figure S8.** $^{13}$C-NMR spectrum (DMSO) of derivative **3d**.

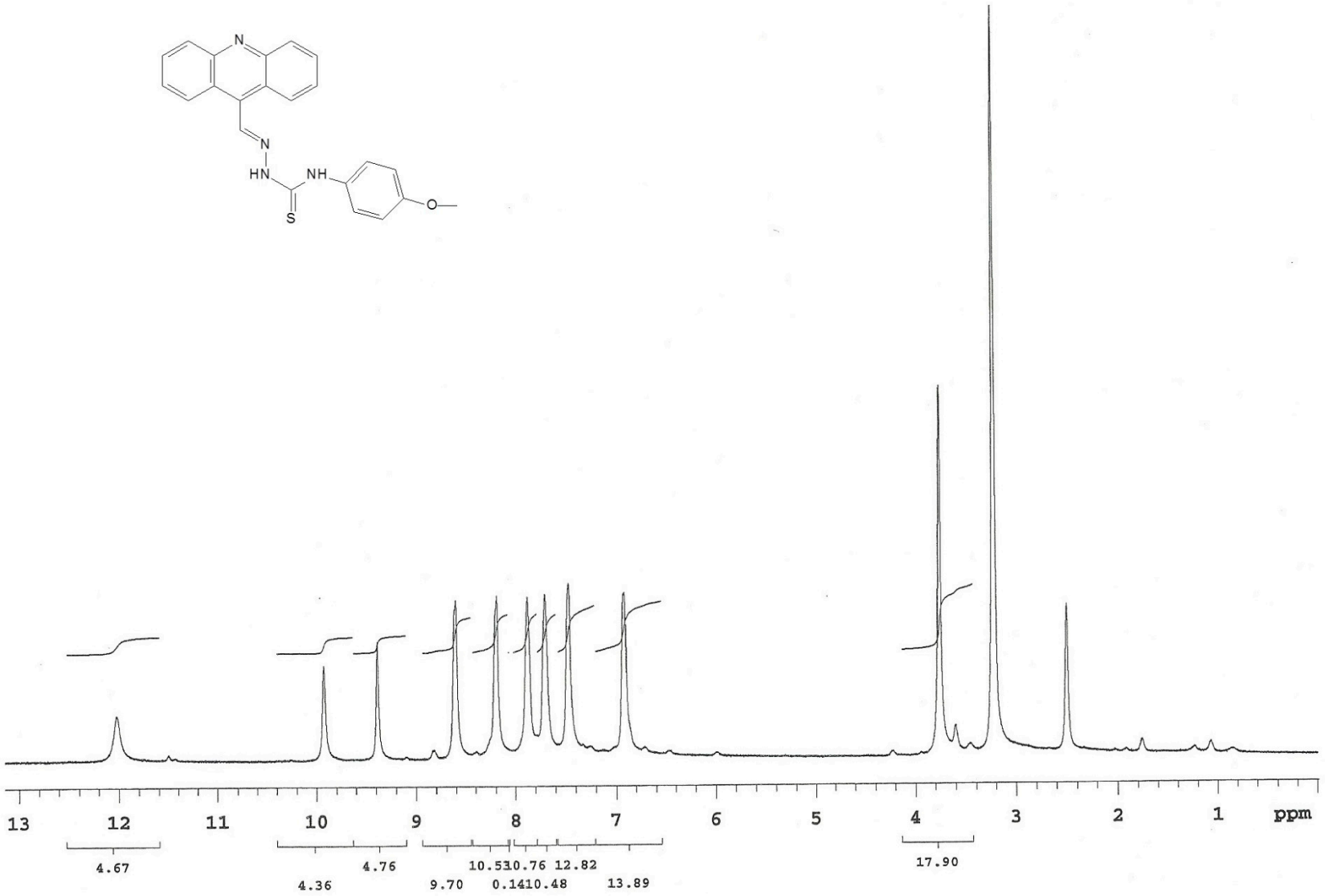


**Figure S9.** $^{1}$H-NMR spectrum (DMSO) of derivative **3e**.

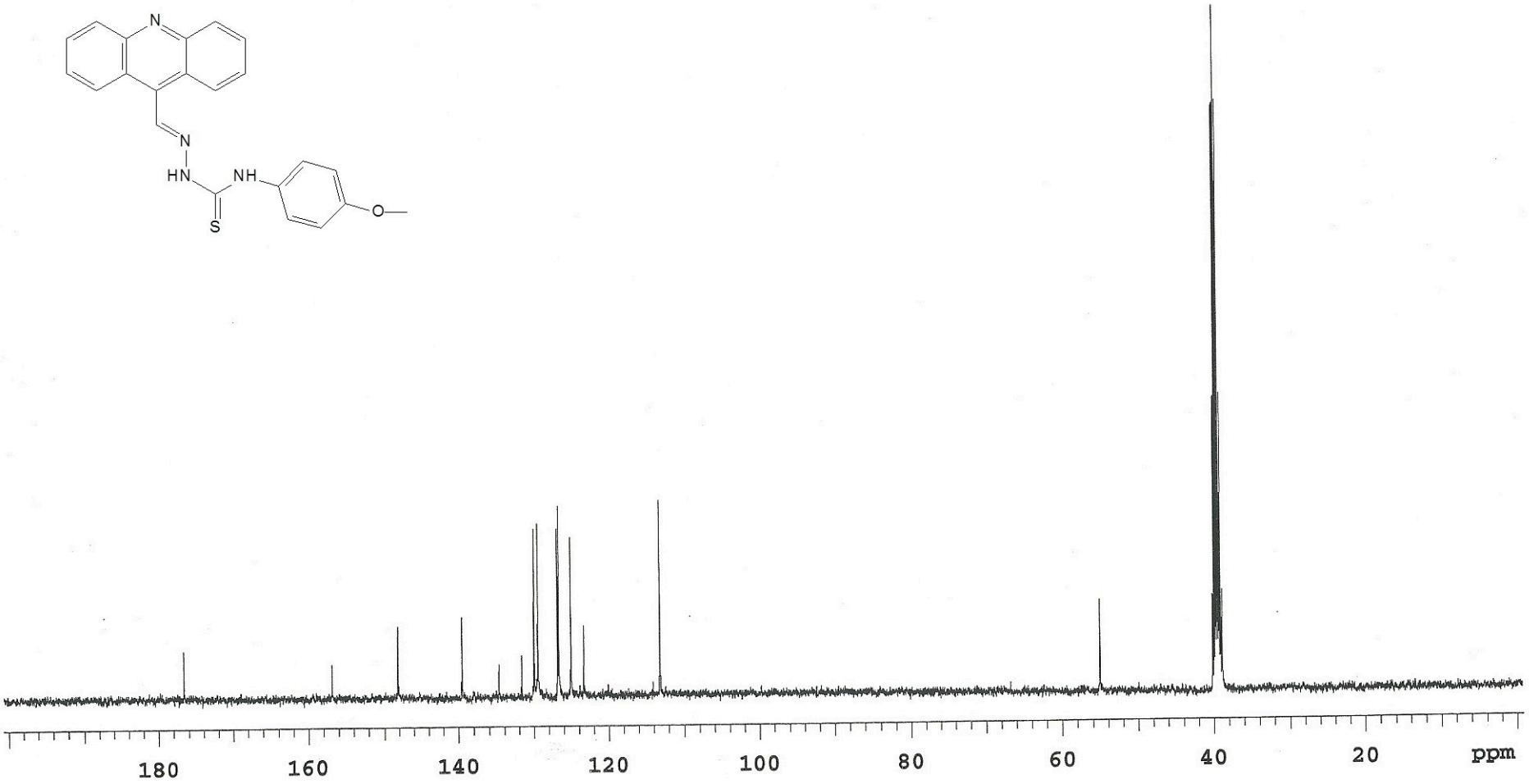


**Figure S10.** $^{13}$C-NMR spectrum (DMSO) of derivative **3e**.

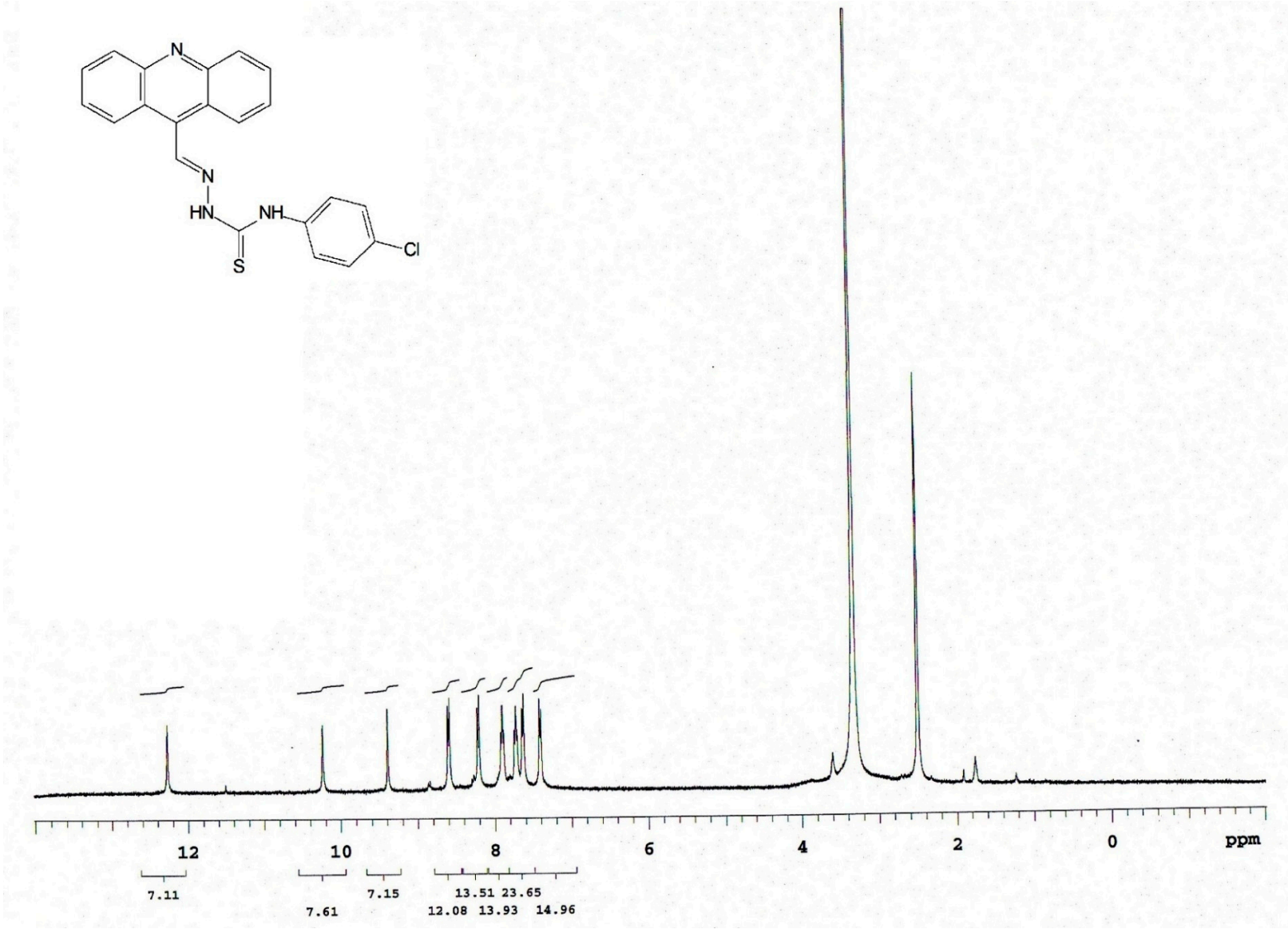


**Figure S11.** $^{1}$H-NMR spectrum (DMSO) of derivative **3f**.

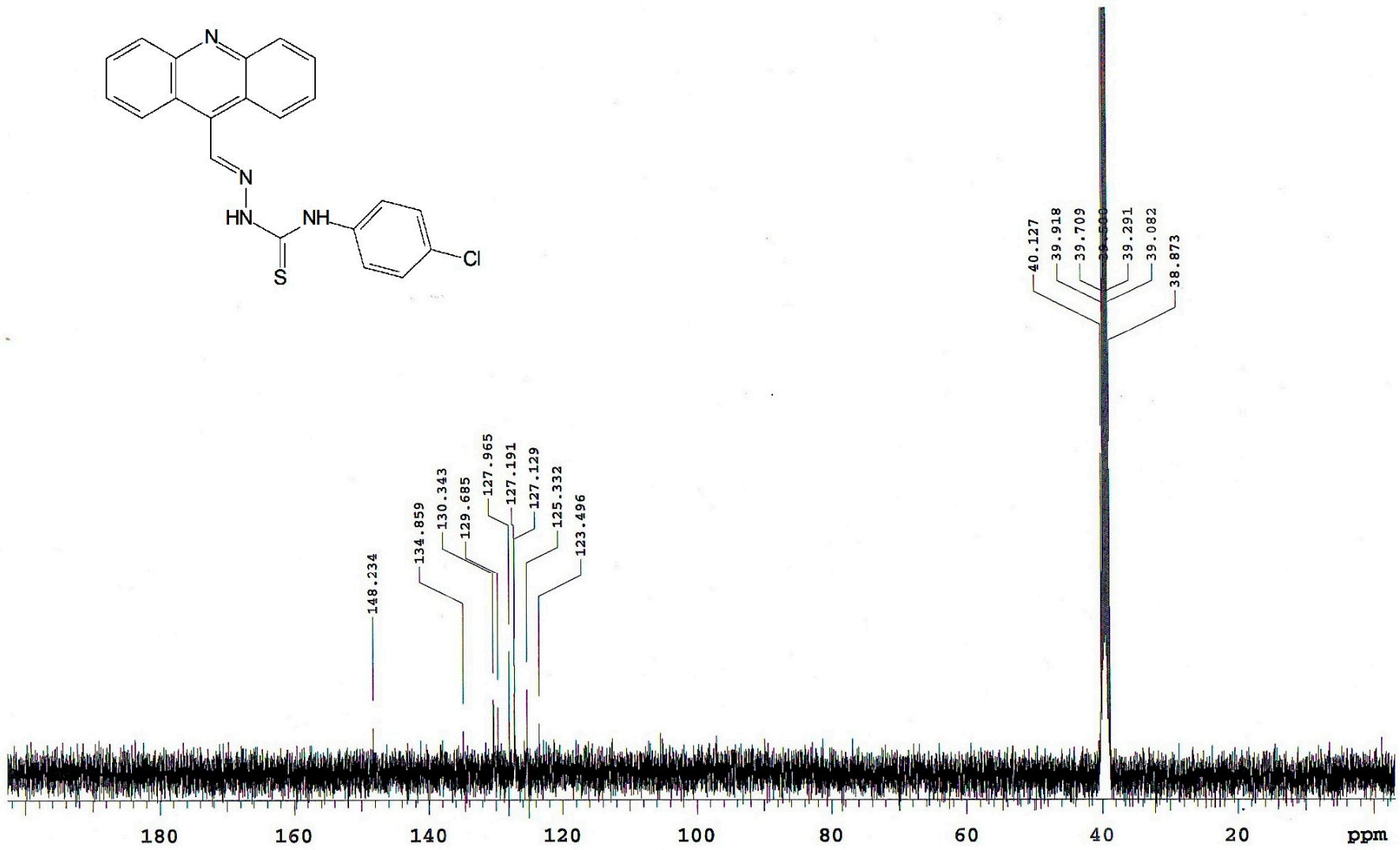


**Figure S12.** $^{13}$C-NMR spectrum (DMSO) of derivative **3f**.

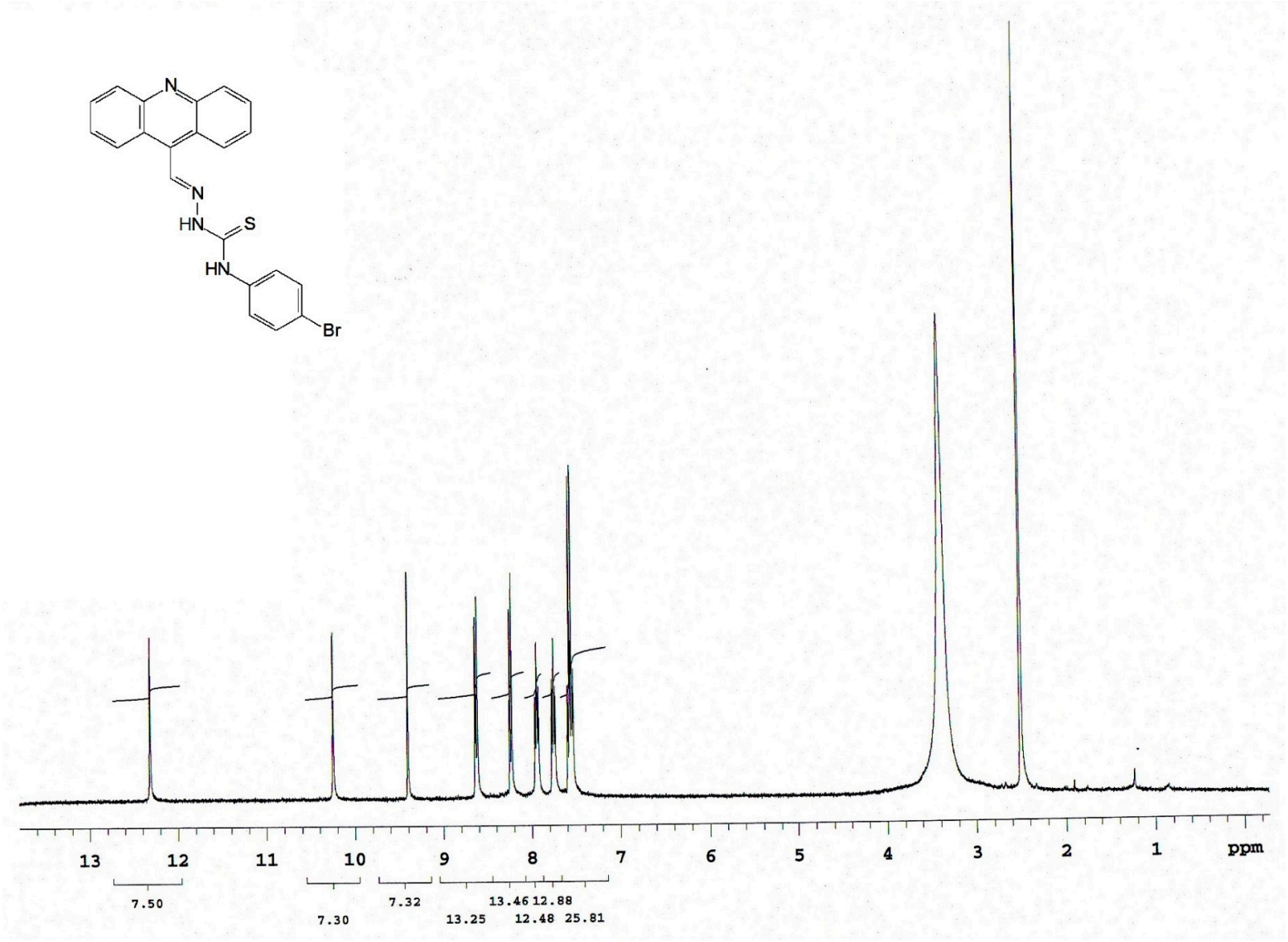


**Figure S13.** $^{1}$H-NMR spectrum (DMSO) of derivative **3g**.

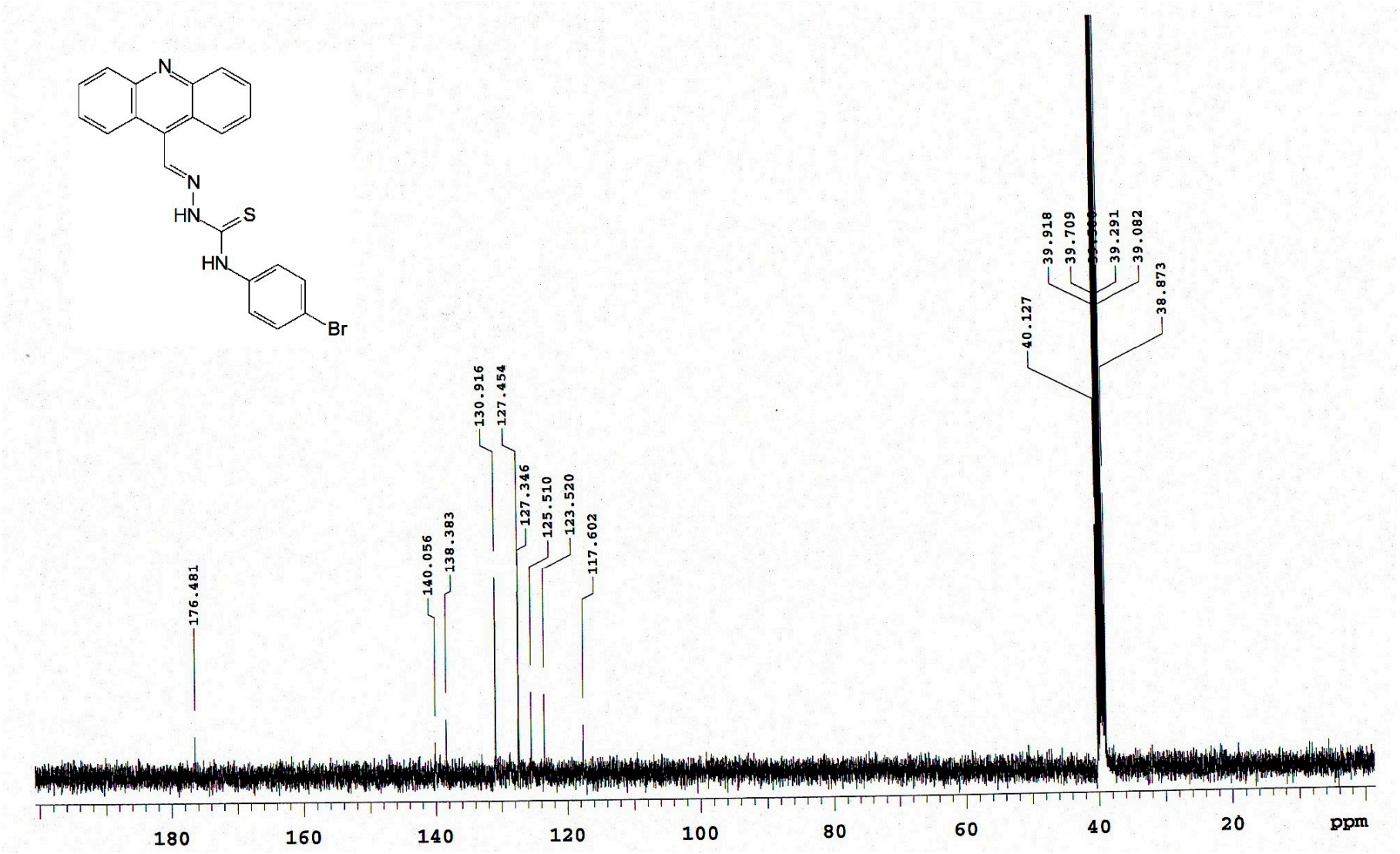


**Figure S14.** $^{13}$C-NMR spectrum (DMSO) of derivative **3g**.

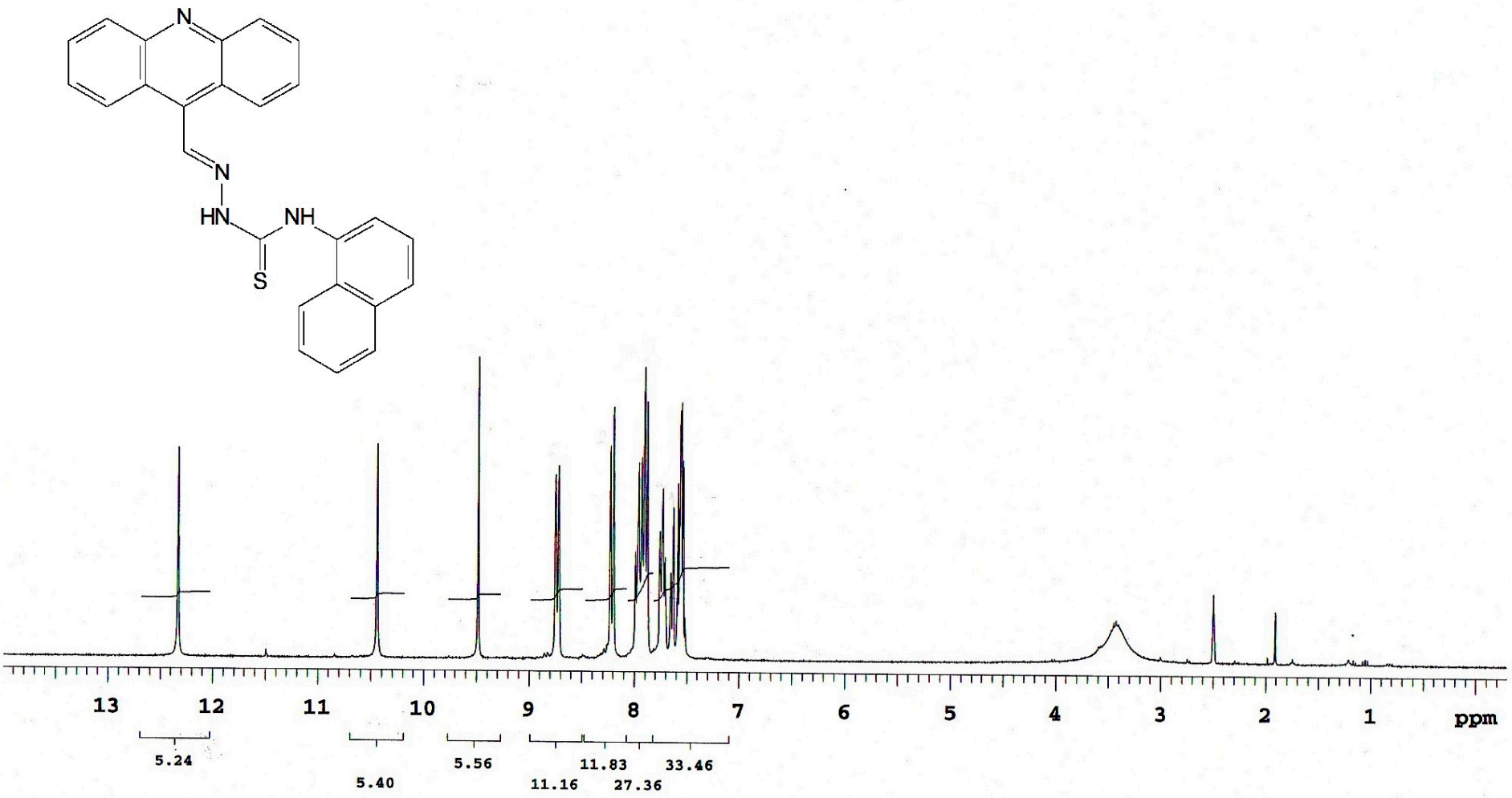


**Figure S15.** $^{1}$H-NMR spectrum (DMSO) of derivative **3h**.

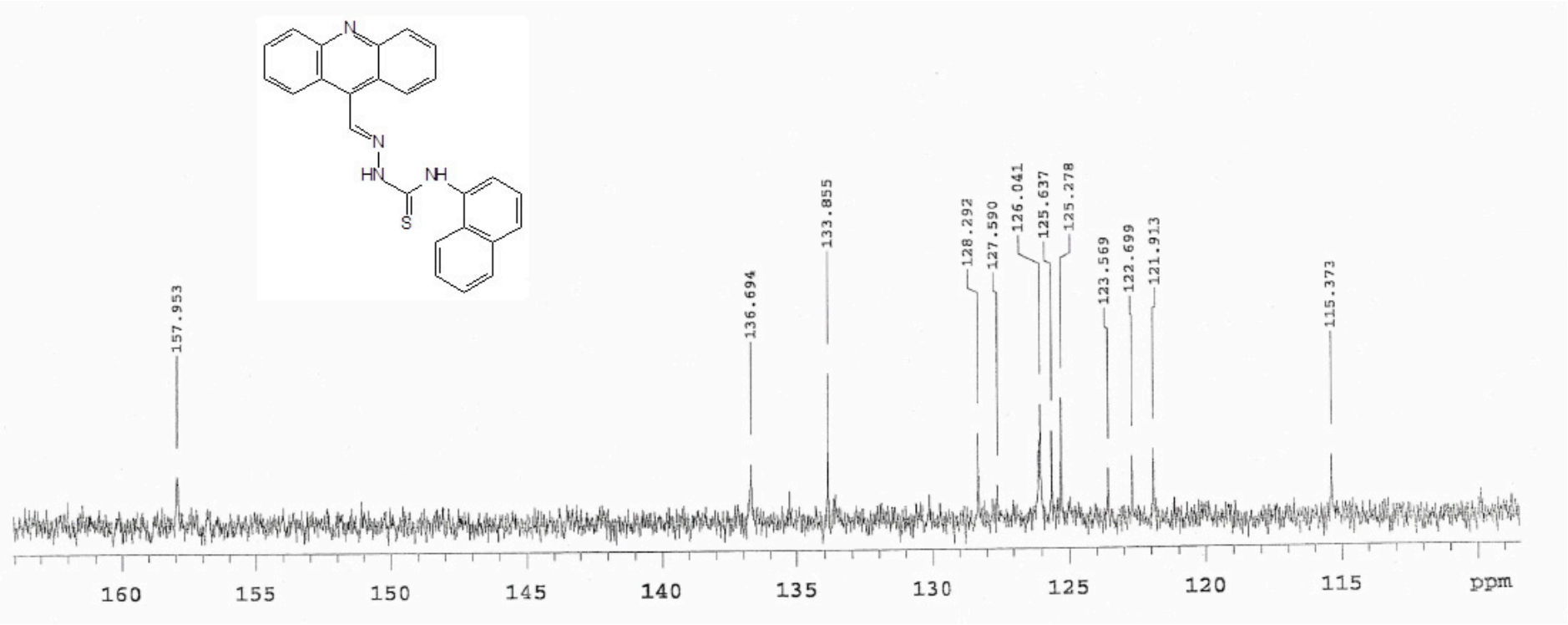


**Figure S16.** $^{13}$C-NMR spectrum (DMSO) of derivative **3h**.

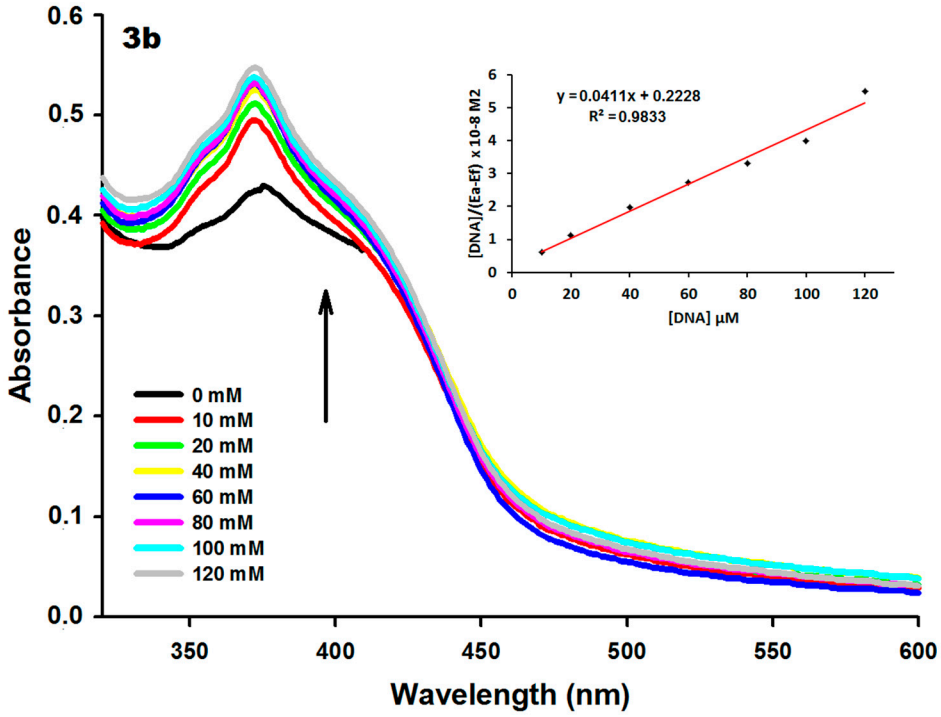


**Figure S17.** Absorption titration of derivative **3b** (50 µM) with increasing concentrations of ctDNA. [DNA] = 0, 10, 20, 40, 60, 80, 100 and 120 µM. Inset: corresponding to the plot of [DNA]/($\varepsilon_a - \varepsilon_f$) as function of DNA concentration as determined from the absorption spectral data. Arrow (↑) refers to hyperchromic effect.

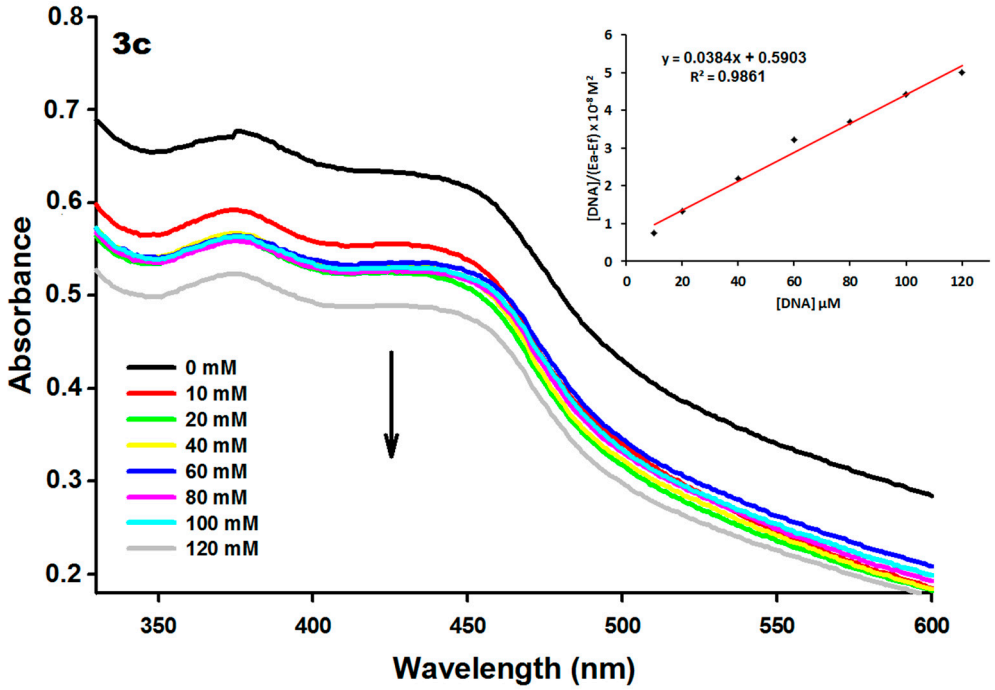


**Figure S18.** Absorption titration of derivative **3c** (50 µM) with increasing concentrations of ctDNA. [DNA] = 0, 10, 20, 40, 60, 80, 100 and 120 µM. Inset: corresponding to the plot of [DNA]/($\varepsilon_a - \varepsilon_f$) as function of DNA concentration as determined from the absorption spectral data. Arrow (↓) refers to hypochromic effect.

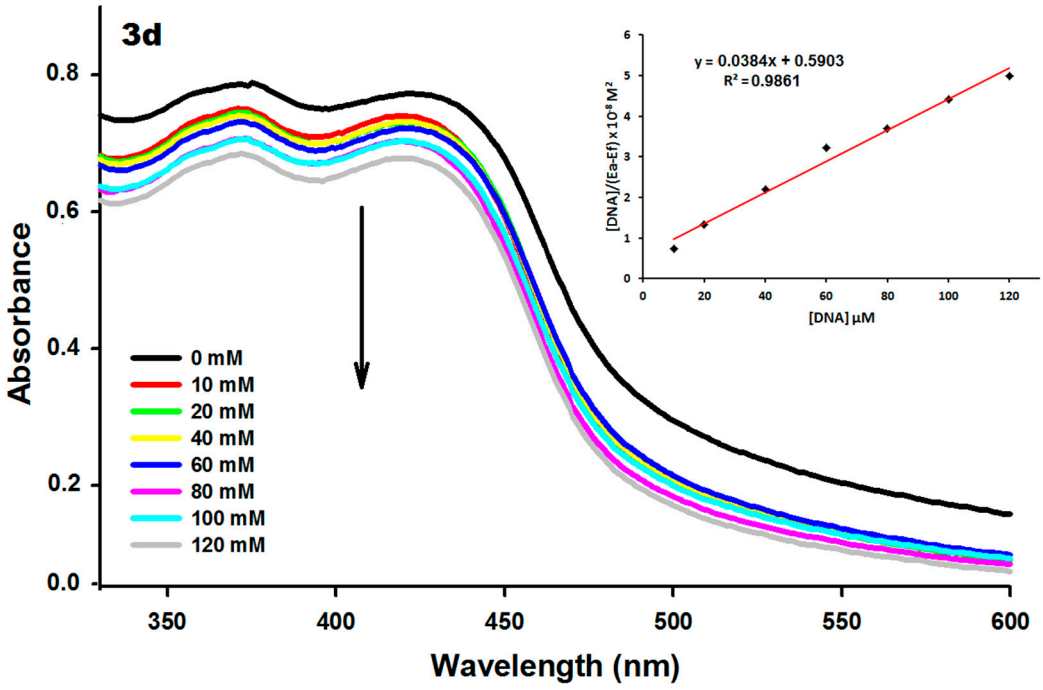


**Figure S19.** Absorption titration of derivative **3d** (50 µM) with increasing concentrations of ctDNA. [DNA] = 0, 10, 20, 40, 60, 80, 100 and 120 µM. Inset: corresponding to the plot of [DNA]/($\varepsilon_a$ − $\varepsilon_f$) as function of DNA concentration as determined from the absorption spectral data. Arrow (↓) refers to hypochromic effect.

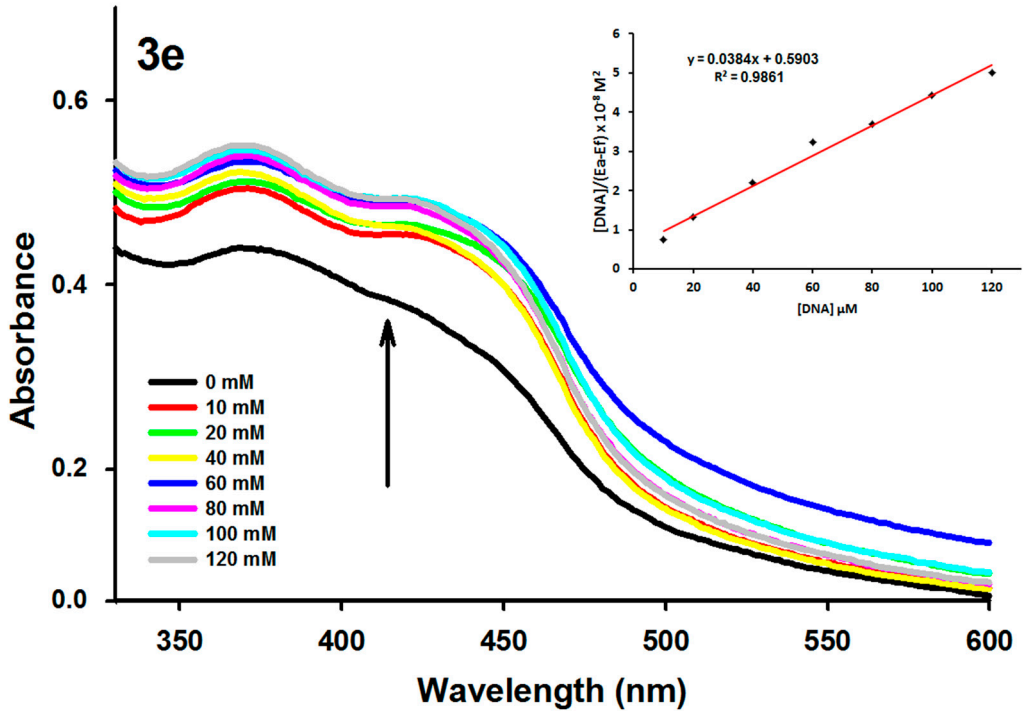


**Figure S20.** Absorption titration of derivative **3e** (50 µM) with increasing concentrations of ctDNA. [DNA] = 0, 10, 20, 40, 60, 80, 100 and 120 µM. Inset: corresponding to the plot of [DNA]/($\varepsilon_a$ − $\varepsilon_f$) as function of DNA concentration as determined from the absorption spectral data. Arrow (↑) refers to hyperchromic effect.

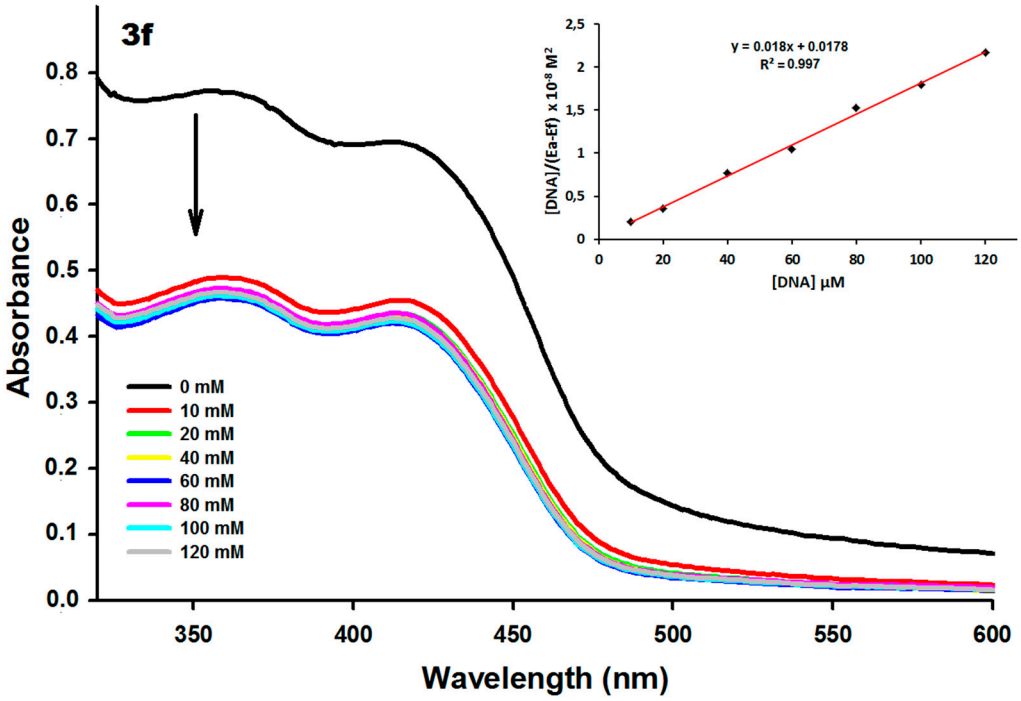


**Figure S21.** Absorption titration of derivative **3f** (50 µM) with increasing concentrations of ctDNA. [DNA] = 0, 10, 20, 40, 60, 80, 100 and 120 µM. Inset: corresponding to the plot of [DNA]/($\varepsilon_a - \varepsilon_f$) as function of DNA concentration as determined from the absorption spectral data. Arrow (↓) refers to hypochromic effect.

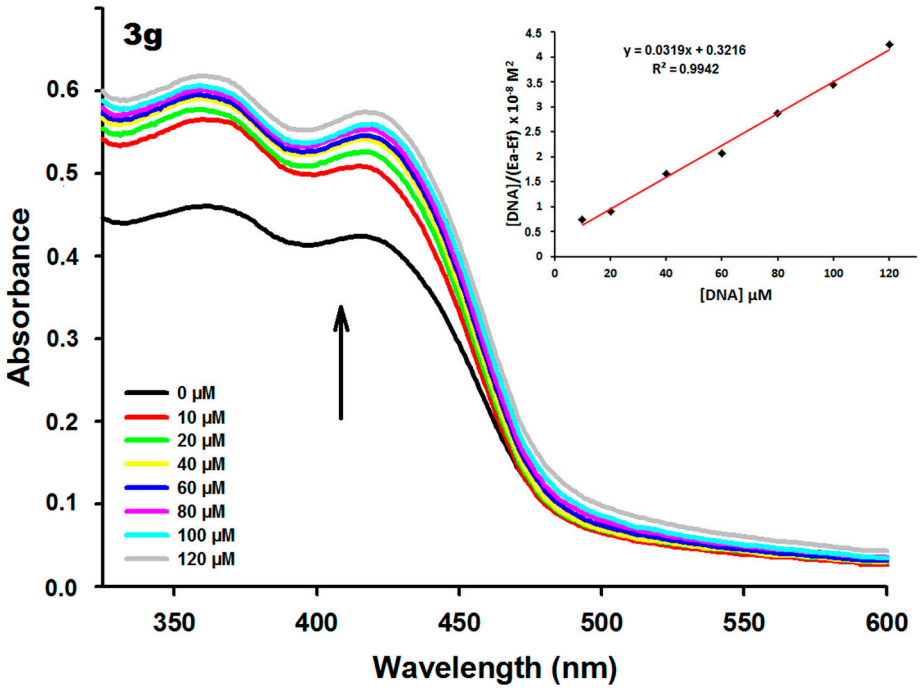


**Figure S22.** Absorption titration of derivative **3g** (50 µM) with increasing concentrations of ctDNA. [DNA] = 0, 10, 20, 40, 60, 80, 100 and 120 µM. Inset: corresponding to the plot of [DNA]/($\varepsilon_a - \varepsilon_f$) as function of DNA concentration as determined from the absorption spectral data. Arrow (↑) refers to hyperchromic effect.

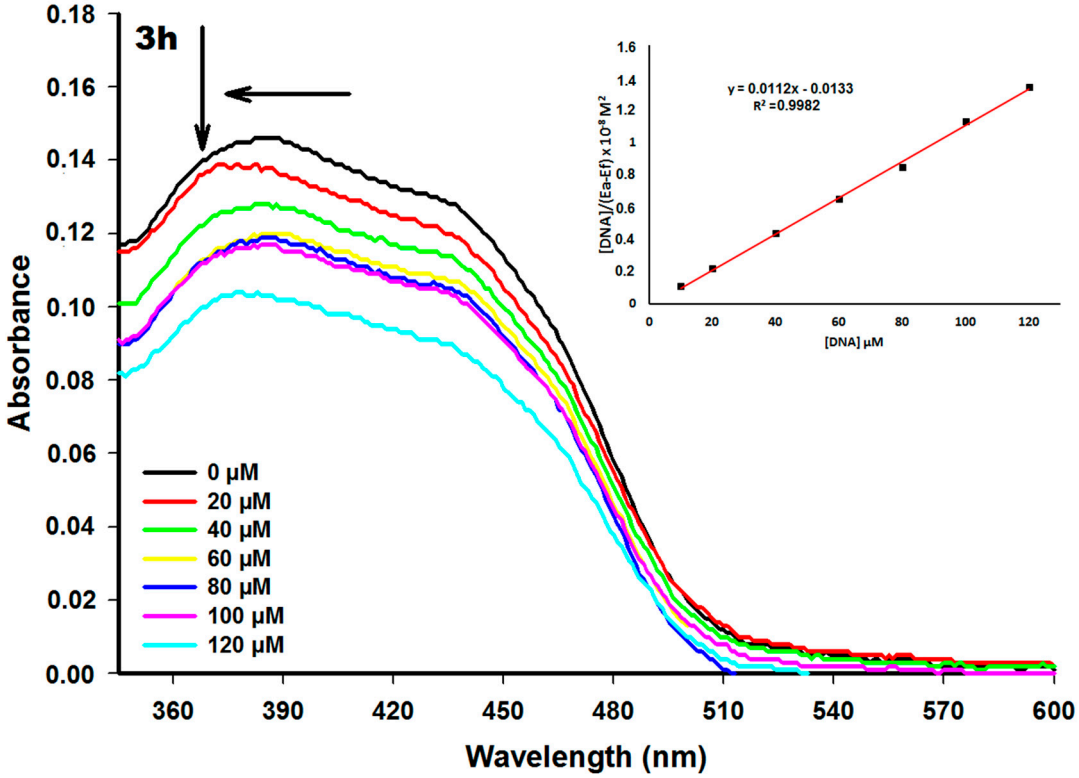


**Figure S23.** Absorption titration of derivative **3h** (50 µM) with increasing concentrations of ctDNA. [DNA] = 0, 10, 20, 40, 60, 80, 100 and 120 µM. Inset: corresponding to the plot of [DNA]/($\varepsilon_a - \varepsilon_f$) as function of DNA concentration as determined from the absorption spectral data. Arrows (↓) and (←) refer to hypochromic, and hypsochromic effects, respectively.

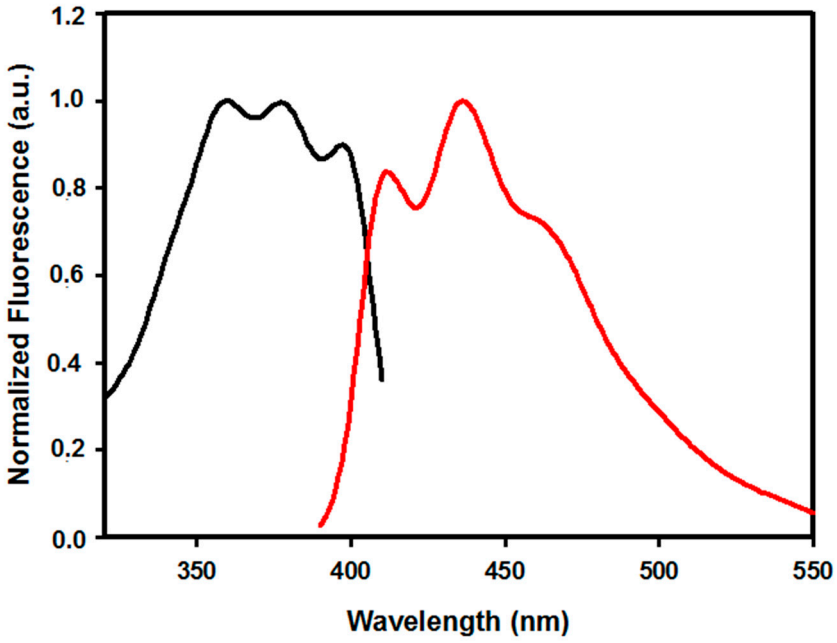


**Figure S24.** Excitation (black) and emission (red) spectra of derivative **3a** at concentrations of 15 µM in Tris-HCl buffer. Excitation at 359 nm and emission at 439 nm.

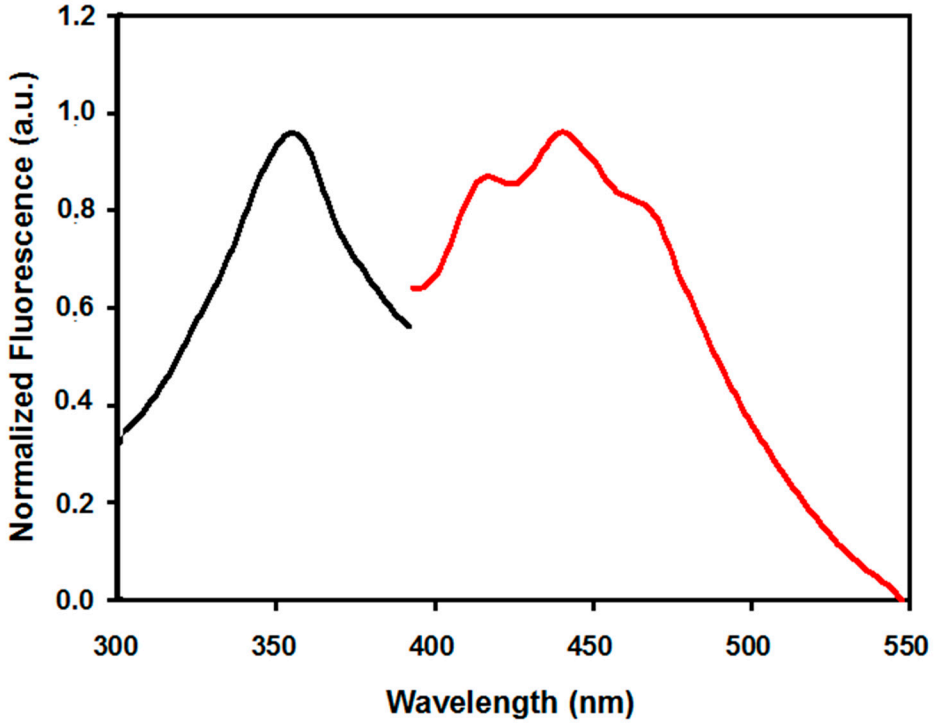


**Figure S25.** Excitation (black) and emission (red) spectra of derivative **3b** at concentrations of 15 μM in Tris-HCl buffer. Excitation at 370 nm and emission at 441 nm.

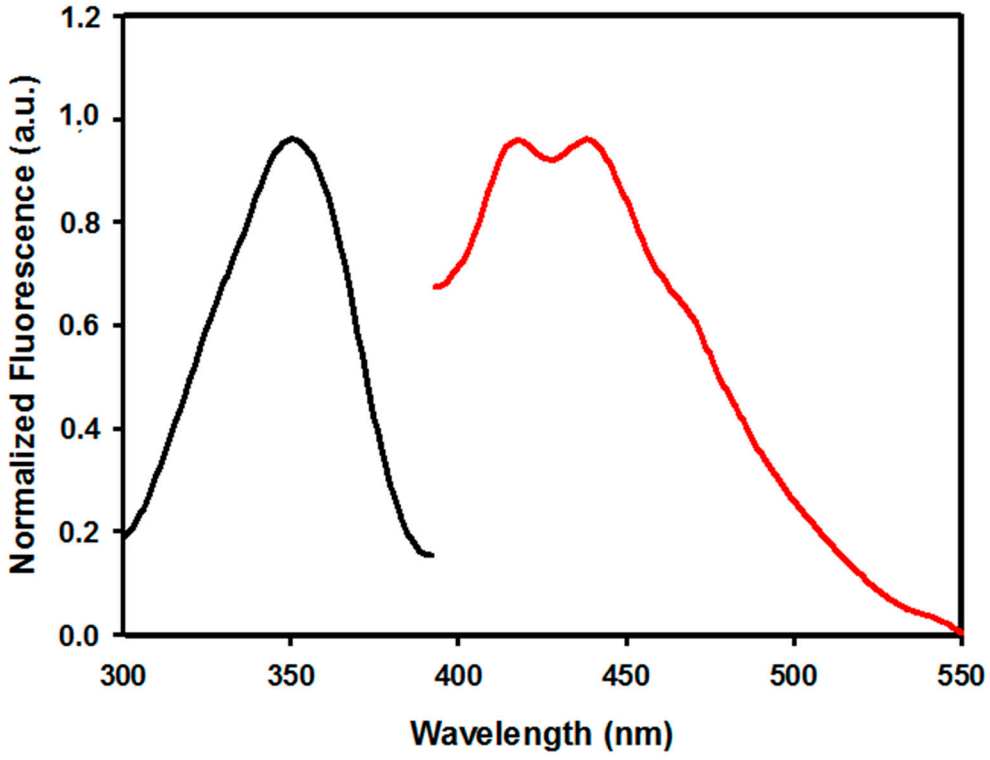


**Figure S26.** Excitation (black) and emission (red) spectra of derivative **3c** at concentrations of 15 μM in Tris-HCl buffer. Excitation at 370 nm and emission at 440 nm.

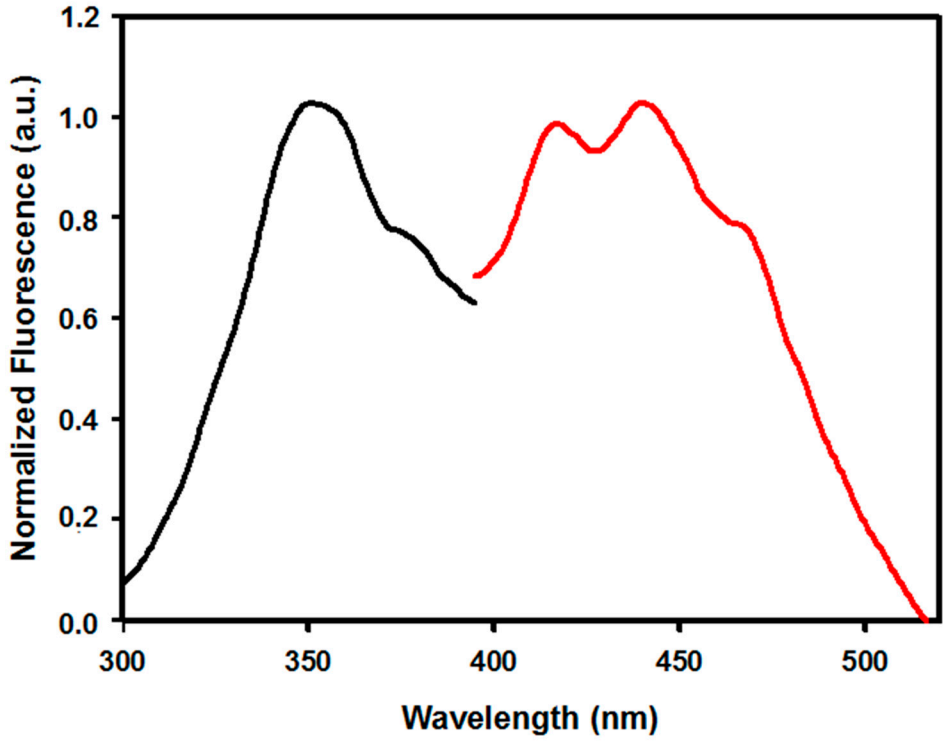


**Figure S27.** Excitation (black) and emission (red) spectra of derivative **3d** at concentrations of 15 μM in Tris-HCl buffer. Excitation at 370 nm and emission at 441 nm.

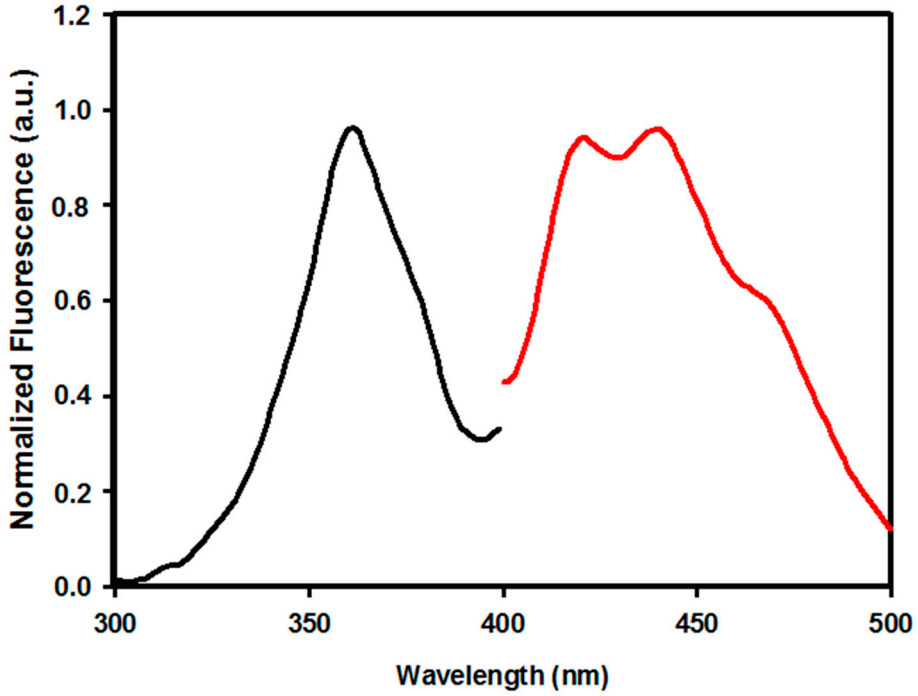


**Figure S28.** Excitation (black) and emission (red) spectra of derivative **3e** at concentrations of 15 μM in Tris-HCl buffer. Excitation at 361 nm and emission at 441 nm.

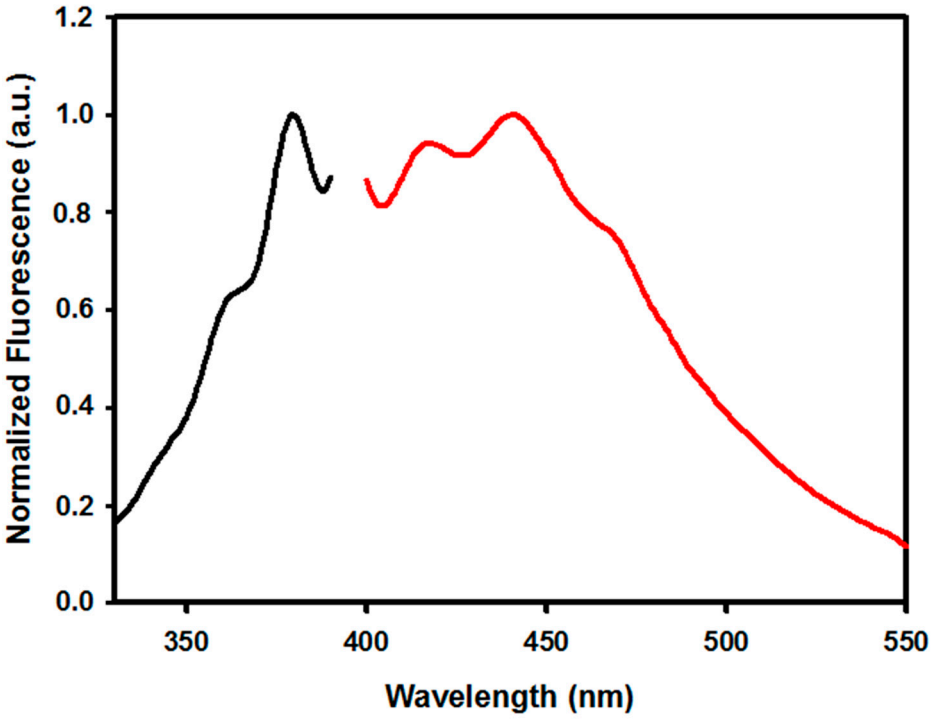


**Figure S29.** Excitation (black) and emission (red) spectra of derivative **3f** at concentrations of 15 µM in Tris-HCl buffer. Excitation at 355 nm and emission at 440 nm.

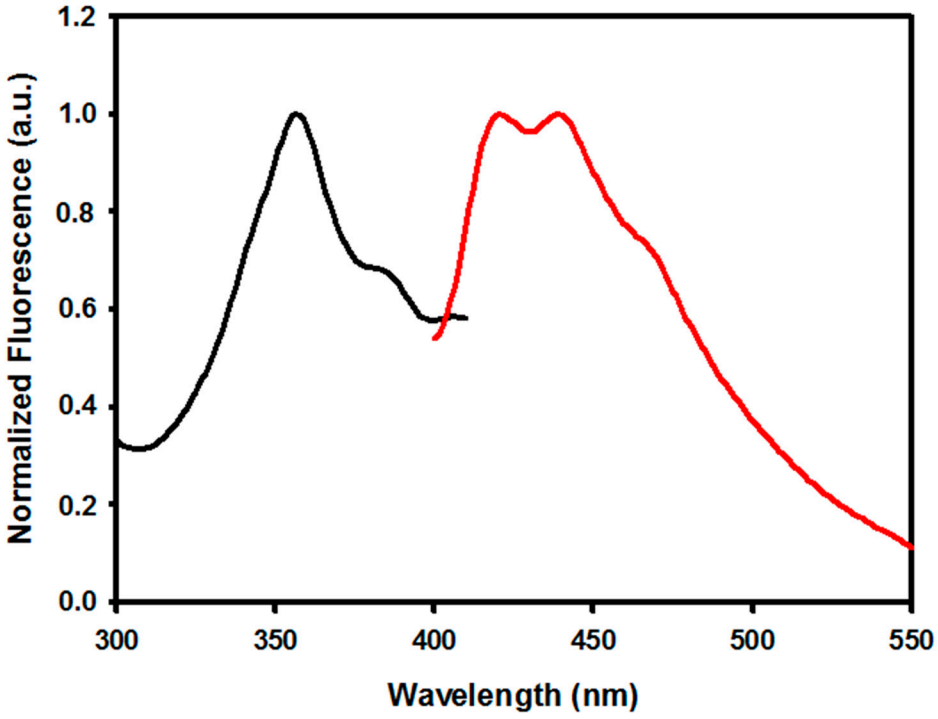


**Figure S30.** Excitation (black) and emission (red) spectra of derivative **3g** at concentrations of 15 µM in Tris-HCl buffer. Excitation at 352 nm and emission at 439 nm.

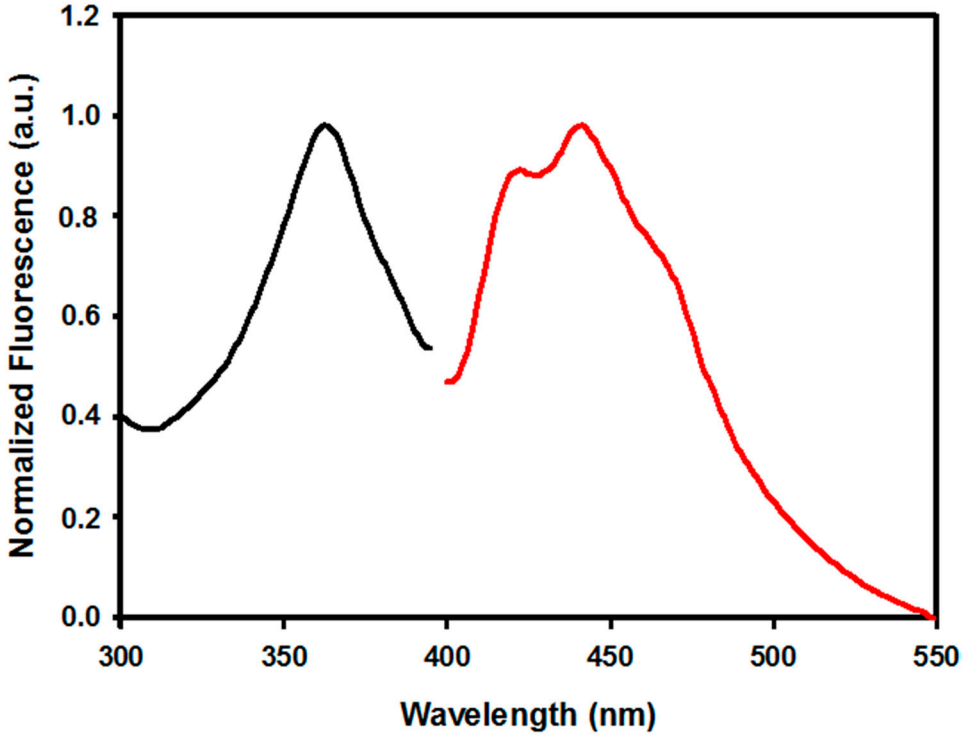


**Figure S31.** Excitation (black) and emission (red) spectra of derivative **3h** at concentrations of 15 µM in Tris-HCl buffer. Excitation at 350 nm and emission at 439 nm.

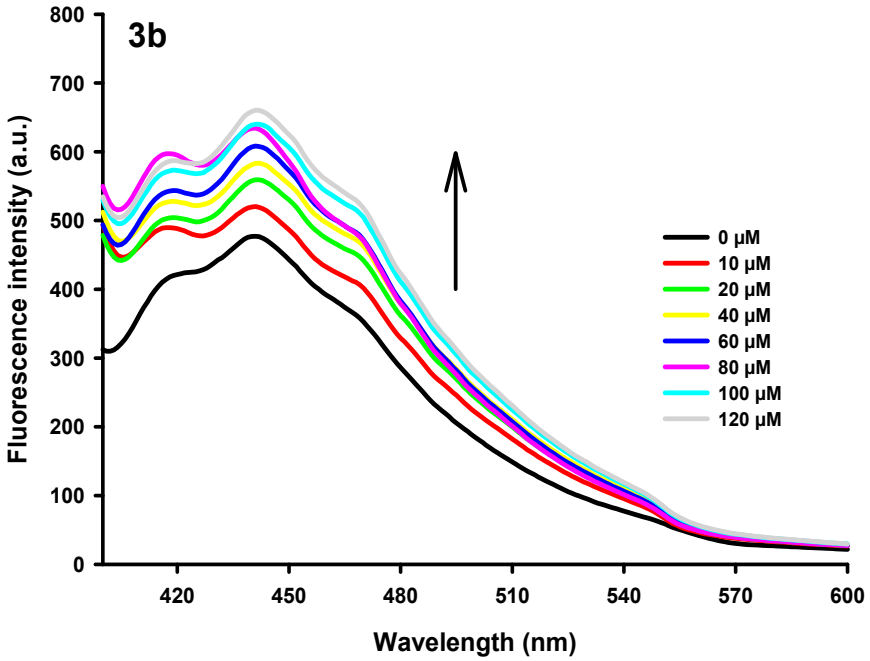


**Figure S32.** Fluorescence spectra of derivative **3b** (15 µM) with increasing concentrations of ctDNA. [DNA] = 0 (gray), 0 (black), 20 (red), 40 (green), 60 (yellow), 80 (dark blue), 100 (pink) and 120 (light blue). Arrow (↑) refers to hyperchromic effect.

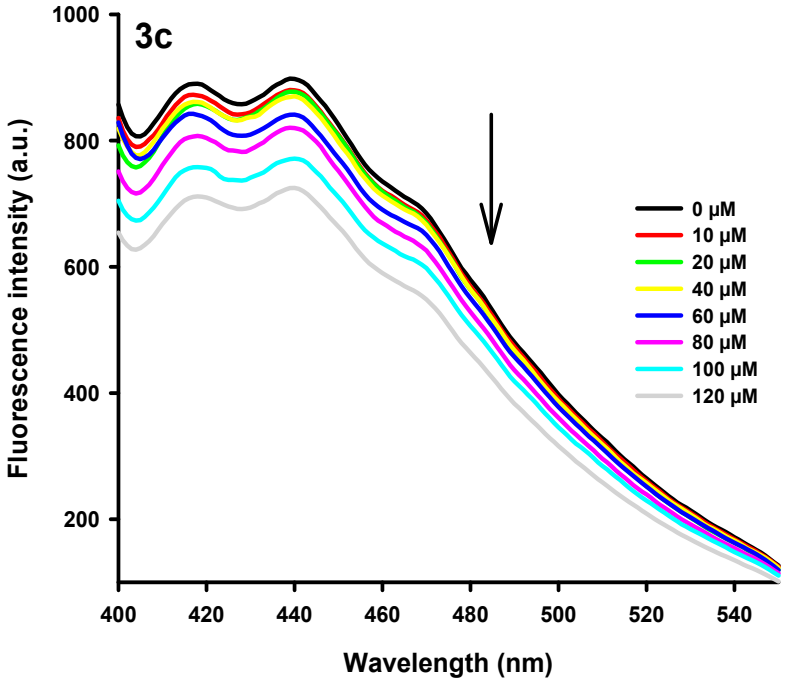


**Figure S33.** Fluorescence spectra of derivative **3c** (15 μM) with increasing concentrations of ctDNA. [DNA] = 0 (gray), 0 (black), 20 (red), 40 (green), 60 (yellow), 80 (dark blue), 100 (pink) and 120 (light blue). Arrow (↓) refers to hypochromic effect.

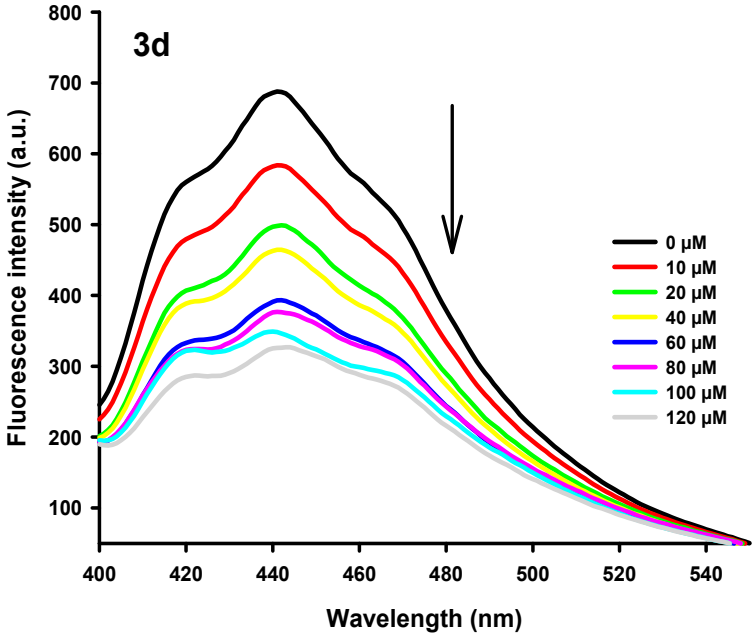


**Figure S34.** Fluorescence spectra of derivative **3d** (15 μM) with increasing concentrations of ctDNA. [DNA] = 0 (gray), 0 (black), 20 (red), 40 (green), 60 (yellow), 80 (dark blue), 100 (pink) and 120 (light blue). Arrow (↓) refers to hypochromic effect.

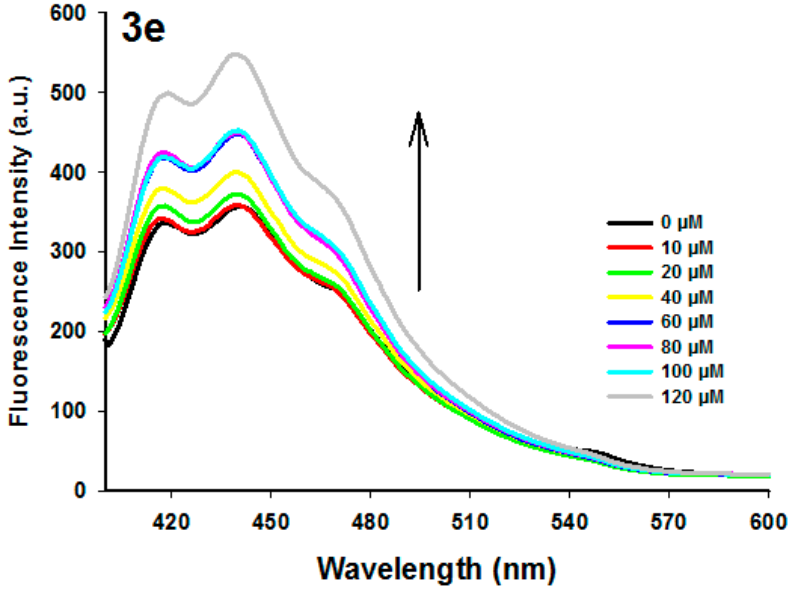


**Figure S35.** Fluorescence spectra of derivative **3e** (15 µM) with increasing concentrations of ctDNA. [DNA] = 0 (gray), 0 (black), 20 (red), 40 (green), 60 (yellow), 80 (dark blue), 100 (pink) and 120 (light blue). Arrow (↑) refers to hyperchromic effect.

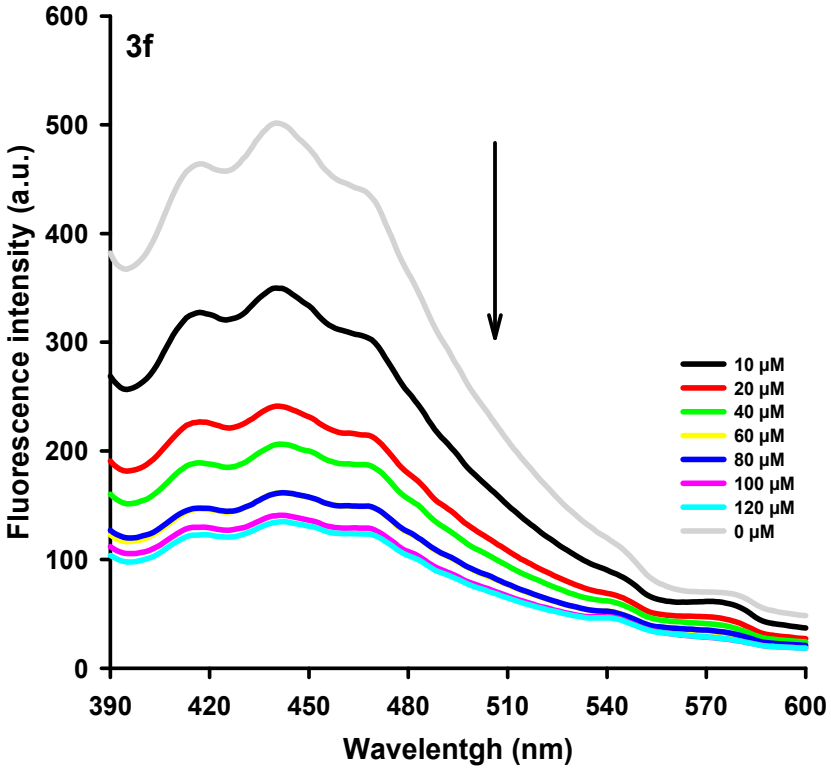


**Figure S36.** Fluorescence spectra of derivative **3f** (15 µM) with increasing concentrations of ctDNA. [DNA] = 0 (gray), 0 (black), 20 (red), 40 (green), 60 (yellow), 80 (dark blue), 100 (pink) and 120 (light blue). Arrow (↓) refers to hypochromic effect.

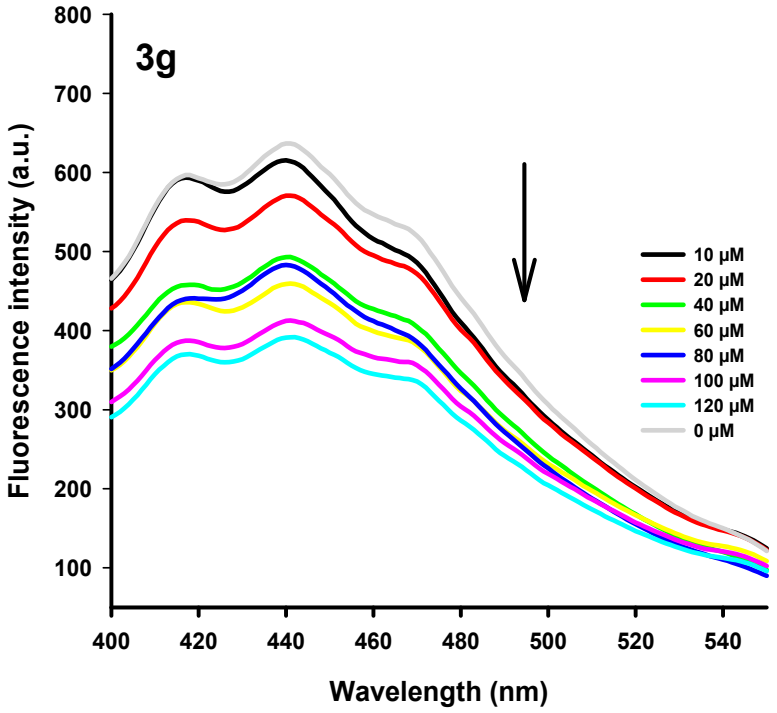


**Figure S37.** Fluorescence spectra of derivative **3g** (15 μM) with increasing concentrations of ctDNA. [DNA] = 0 (gray), 0 (black), 20 (red), 40 (green), 60 (yellow), 80 (dark blue), 100 (pink) and 120 (light blue). Arrow (↓) refers to hypochromic effect.

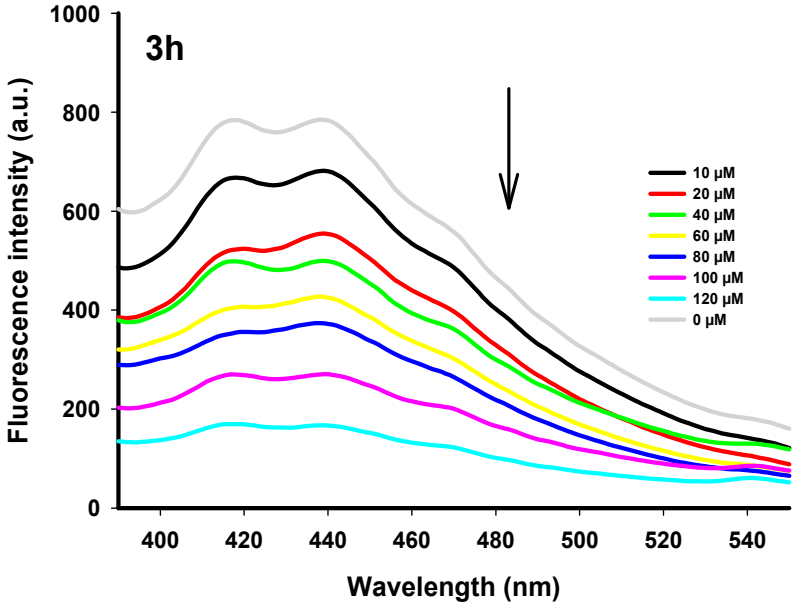


**Figure S38.** Fluorescence spectra of derivative **3h** (15 μM) with increasing concentrations of ctDNA. [DNA] = 0 (gray), 0 (black), 20 (red), 40 (green), 60 (yellow), 80 (dark blue), 100 (pink) and 120 (light blue). Arrow (↓) refers to hypochromic effect.

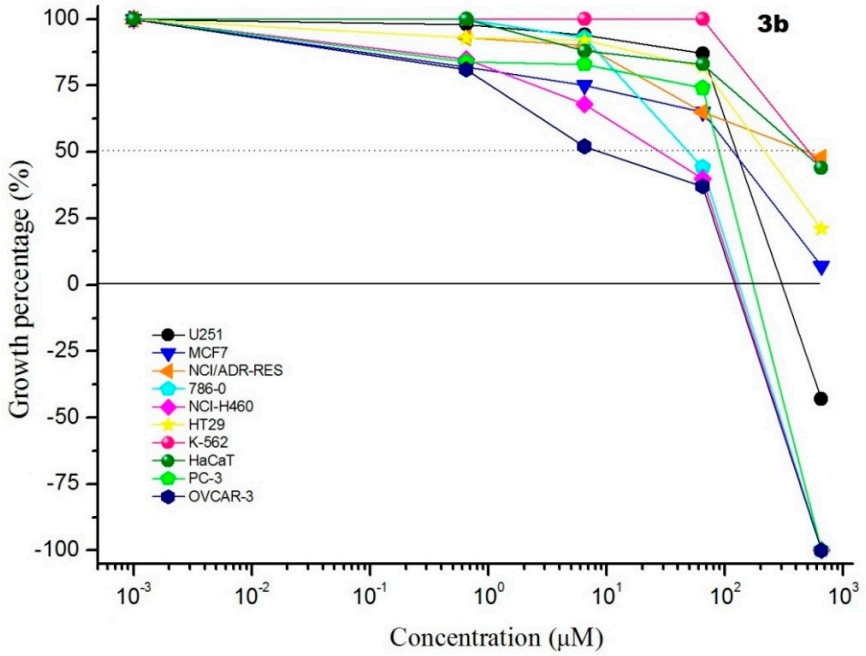


**Figure S39.** Antiproliferative activity of **3b** against nine cancerous cell lines: U251 (glioma, SNC); MCF-7 (breast adenocarcinoma); NCI-ADR/RES (ovary, multidrug resistance phenotype); 786-0 (kidney); NCI-H460 (lung non-small cell adenocarcinoma); PC-3 (prostate); OVCAR-3 (ovary); HT-29 (colon); K-562 (Chronic myeloid leukemia) and human keratinocytes (HaCaT).

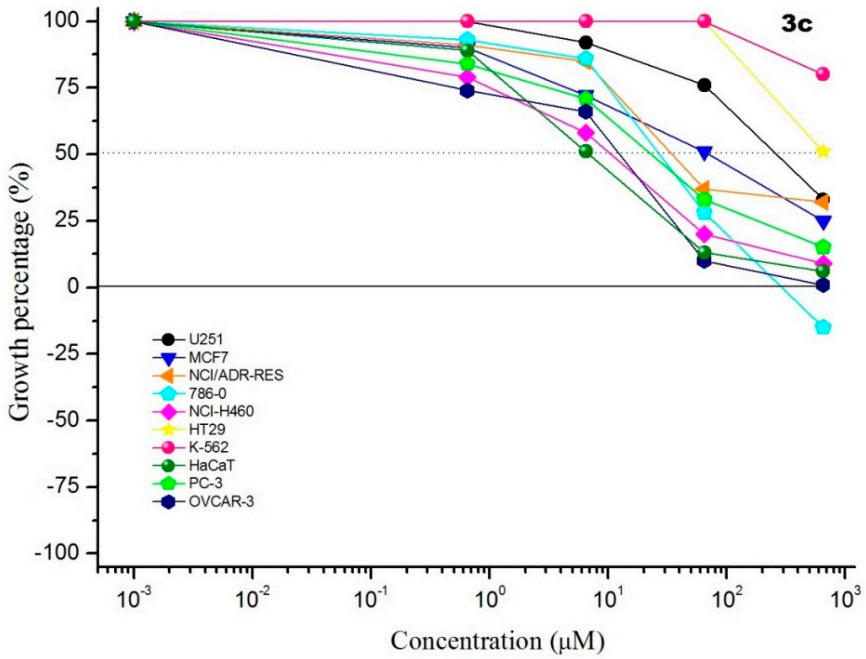


**Figure S40.** Antiproliferative activity of **3c** against nine cancerous cell lines: U251 (glioma, SNC); MCF-7 (breast adenocarcinoma); NCI-ADR/RES (ovary, multidrug resistance phenotype); 786-0 (kidney); NCI-H460 (lung non-small cell adenocarcinoma); PC-3 (prostate); OVCAR-3 (ovary); HT-29 (colon); K-562 (Chronic myeloid leukemia) and human keratinocytes (HaCaT).

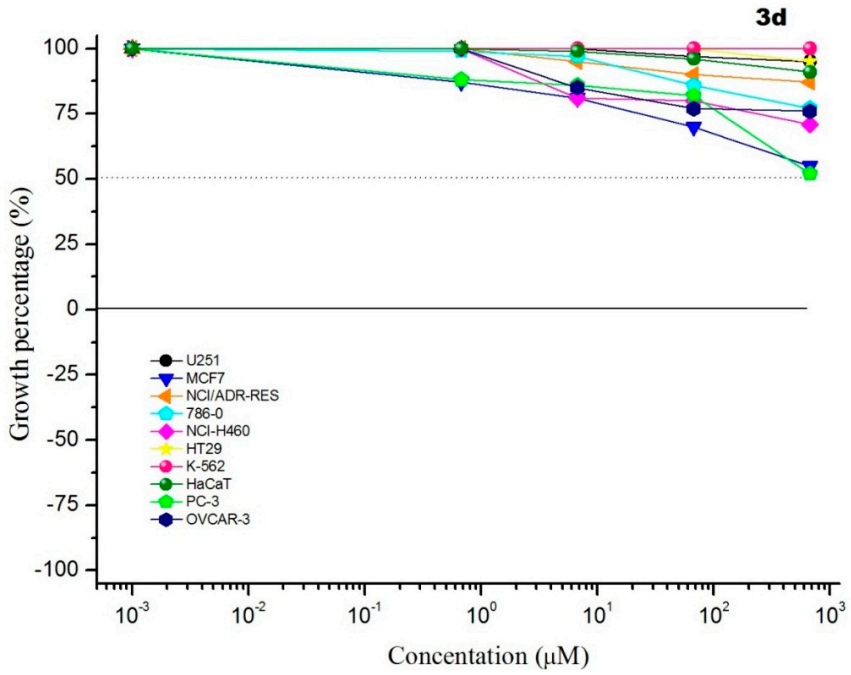


**Figure S41.** Antiproliferative activity of **3d** against nine cancerous cell lines: U251 (glioma, SNC); MCF-7 (breast adenocarcinoma); NCI-ADR/RES (ovary, multidrug resistance phenotype); 786-0 (kidney); NCI-H460 (lung non-small cell adenocarcinoma); PC-3 (prostate); OVCAR-3 (ovary); HT-29 (colon); K-562 (Chronic myeloid leukemia) and human keratinocytes (HaCaT).

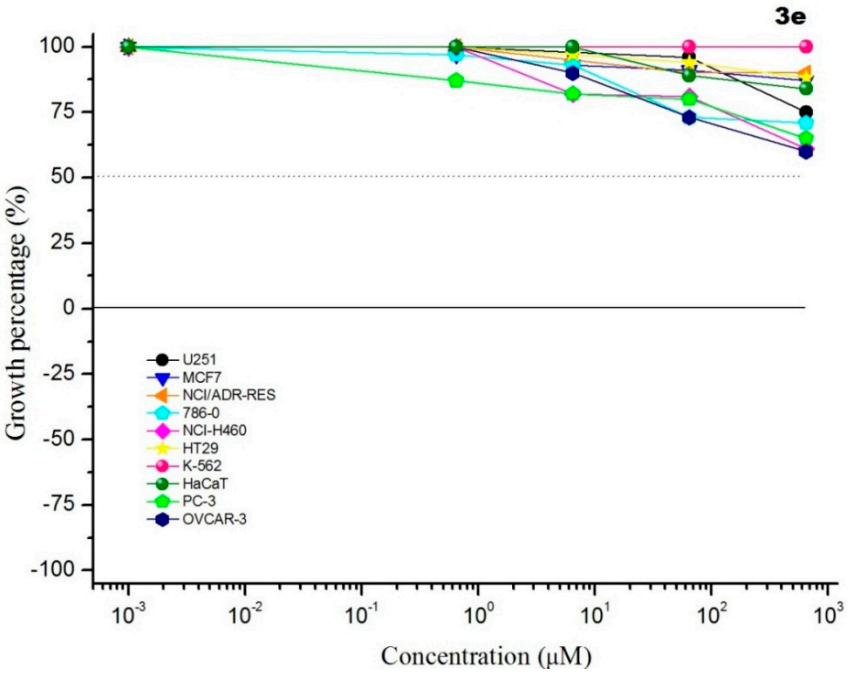


**Figure S42.** Antiproliferative activity of **3e** against nine cancerous cell lines: U251 (glioma, SNC); MCF-7 (breast adenocarcinoma); NCI-ADR/RES (ovary, multidrug resistance phenotype); 786-0 (kidney); NCI-H460 (lung non-small cell adenocarcinoma); PC-3 (prostate); OVCAR-3 (ovary); HT-29 (colon); K-562 (Chronic myeloid leukemia) and human keratinocytes (HaCaT).

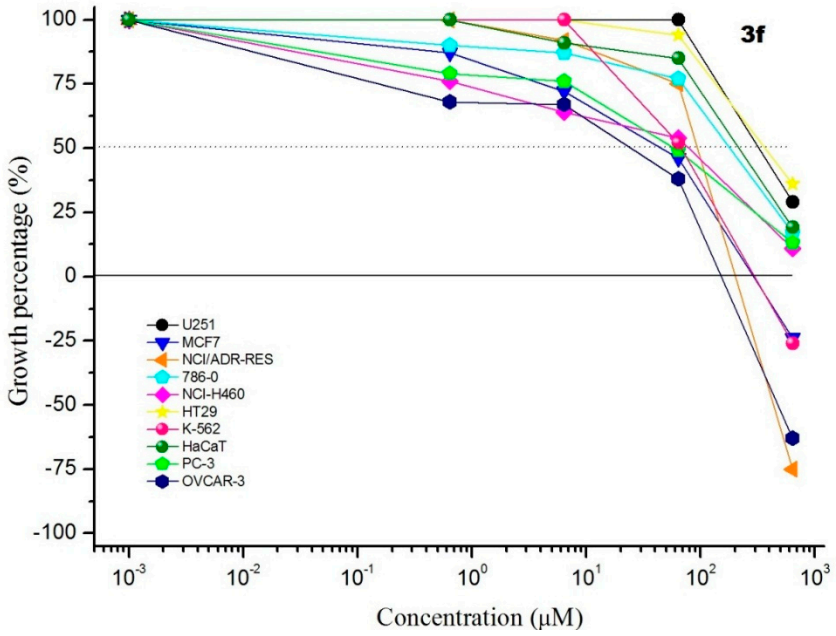


**Figure S43.** Antiproliferative activity of **3f** against nine cancerous cell lines: U251 (glioma, SNC); MCF-7 (breast adenocarcinoma); NCI-ADR/RES (ovary, multidrug resistance phenotype); 786-0 (kidney); NCI-H460 (lung non-small cell adenocarcinoma); PC-3 (prostate); OVCAR-3 (ovary); HT-29 (colon); K-562 (Chronic myeloid leukemia) and human keratinocytes (HaCaT).

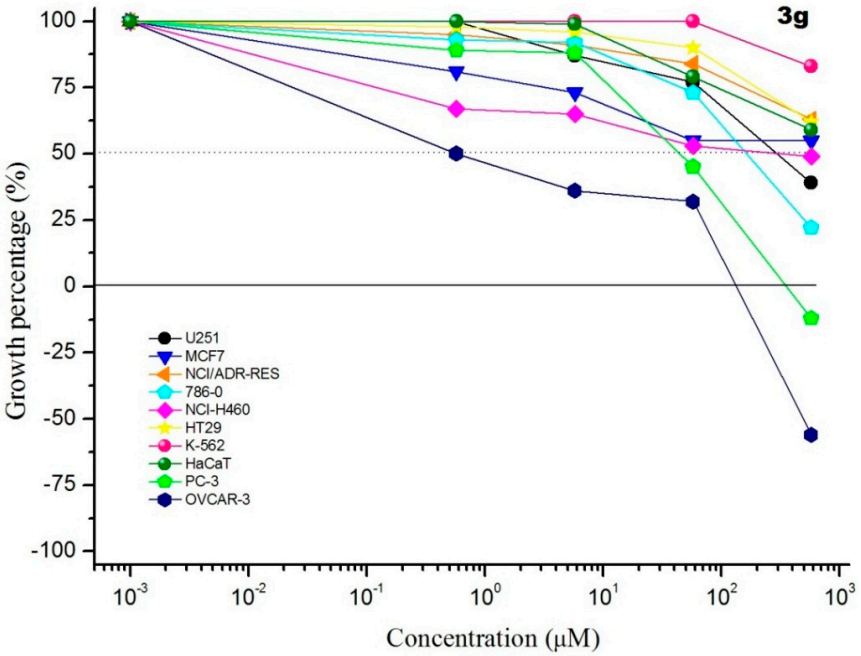


**Figure S44.** Antiproliferative activity of **3g** against nine cancerous cell lines: U251 (glioma, SNC); MCF-7 (breast adenocarcinoma); NCI-ADR/RES (ovary, multidrug resistance phenotype); 786-0 (kidney); NCI-H460 (lung non-small cell adenocarcinoma); PC-3 (prostate); OVCAR-3 (ovary); HT-29 (colon); K-562 (Chronic myeloid leukemia) and human keratinocytes (HaCaT).

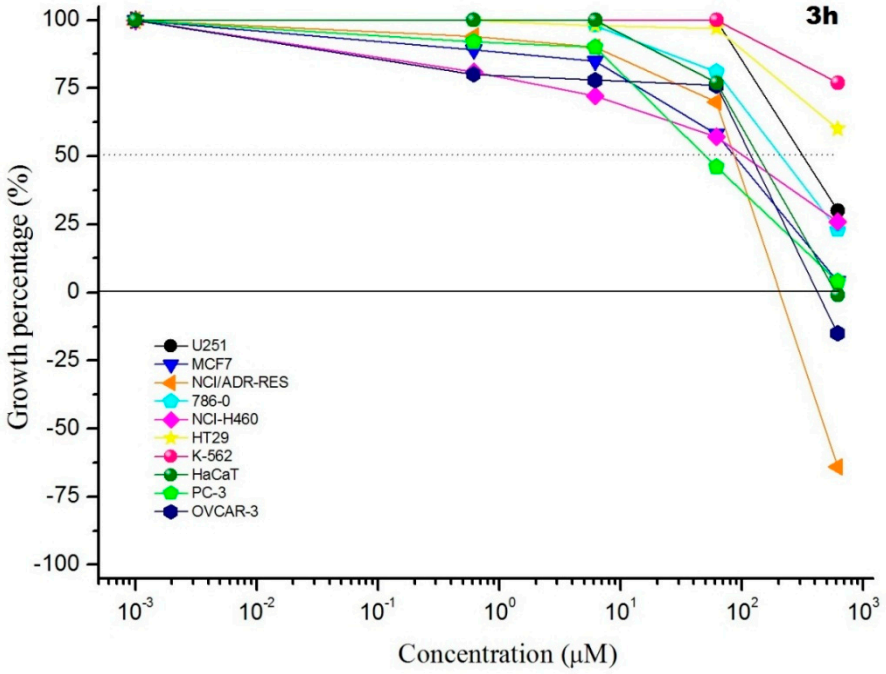


**Figure S45.** Antiproliferative activity of **3h** against nine cancerous cell lines: U251 (glioma, SNC); MCF-7 (breast adenocarcinoma); NCI-ADR/RES (ovary, multidrug resistance phenotype); 786-0 (kidney); NCI-H460 (lung non-small cell adenocarcinoma); PC-3 (prostate); OVCAR-3 (ovary); HT-29 (colon); K-562 (Chronic myeloid leukemia) and human keratinocytes (HaCaT).

**Table S1.** Cell lines used *in vitro* antiproliferative assays and their inoculation densities.

| Cell Lines | Density ($\times 10^4$ cells/mL) |
|---|---|
| U251 (glioma, SNC) | 4.0 |
| MCF-7 (breast adenocarcinoma) | 6.0 |
| NCI-ADR/RES (ovary, multidrug resistance phenotype) | 5.0 |
| 786-O (kidney) | 4.5 |
| NCI-H460 (lung non-small cell adenocarcinoma) | 4.0 |
| PC-3 (prostate) | 4.0 |
| OVCAR-3 (ovary) | 7.0 |
| HT-29 (colon) | 4.0 |
| K-562 (Chronic myeloid leukemia) | 6.0 |
| HaCaT (human keratinocytes) | 4.0 |

**Table S2.** Exact mass, calculated and found *m*/*z* values for compounds (**3a**–**h**).

| Compound | Exact Mass Calculated * | Calculated *m*/*z* ** | Found [M + 1] ** |
|---|---|---|---|
| **3a** | 356.1096 | 356.1096 (100.0%), 357.1129 (22.7%), 358.1054 (4.5%), 358.1163 (2.5%), 357.1066 (1.5%), 359.1087 (1.0%) | 357.124 |
| **3b** | 384.1409 | 384.1409 (100.0%), 385.1442 (24.9%), 386.1367 (4.5%), 386.1476 (3.0%), 385.1379 (1.5%), 387.1400 (1.1%) | 385.134 |
| **3c** | 384.1409 | 384.1409 (100.0%), 385.1442 (24.9%), 386.1367 (4.5%), 386.1476 (3.0%), 385.1379 (1.5%), 387.1400 (1.1%) | 385.131 |
| **3d** | 370.1252 | 370.1252 (100.0%), 371.1286 (23.8%), 372.1210 (4.5%), 372.1319 (2.7%), 371.1223 (1.5%), 373.1224 (1.1%) | 371.120 |
| **3e** | 386.1201 | 386.1201 (100.0%), 387.1235 (23.8%), 388.1159 (4.5%), 388.1268 (2.7%), 387.1172 (1.5%), 389.1193 (1.1%) | 387.073 |
| **3f** | 390.0706 | 390.0706 (100.0%), 392.0676 (32.0%), 391.0739 (22.7%), 393.0710 (7.3%), 392.0664 (4.5%), 392.0773 (2.5%), 391.0676 (1.5%), 394.0634 (1.4%), 393.0697 (1.0%) | 391.041 |
| **3g** | 434.0201 | 434.0201 (100.0%), 436.0180 (97.3%), 435.0234 (22.7%), 437.0214 (22.1%), 436.0159 (4.5%), 438.0138 (4.4%), 436.0268 (2.5 %), 438.0247 (2.4%), 435.0107 (1.5%), 437.0151 (1.4%), 437.0192 (1.0%) | 436.968 |
| **3h** | 406.1252 | 406.1252 (100.0%), 407.1286 (27.0%), 408.1210 (4.5%), 408.1319 (3.5%), 407.1223 (1.5%), 409.1244 (1.2%) | 407.024 |

***** The values were calculated using the software ChemDraw 12 (PerkinElmer Informatics, Waltham, MA, USA); ****** The values corresponding to found molecular ions mass and match to the secondary calculated *m*/*z* peaks. Mass spectra were recorded on matrix-assisted laser desorption/ionization recorded with a time-of-flight mass spectrometer (MALDI-TOF).